https://doi.org/10.5194/egusphere-2026-1307
Preprint. Discussion started: 1 April 2026


# SLUCM+BEM (v2.0): implementing a prognostic indoor temperature scheme for application to global cities

Yuya Takane[1], Yukihiro Kikegawa[2], Zhiwen Luo[3], Hiroyuki Kusaka[4], Sue Grimmond[5]

[1]Center for Climate Change Adaptation, National Institute for Environmental Studies, Tsukuba, 305-8506, Japan
[2]School of Science and Engineering, Meisei University, Tokyo, 191-8506, Japan
[3]Welsh School of Architecture, Cardiff University, Cardiff, CF10 3NB, UK
[4]Center for Computational Sciences, University of Tsukuba, Tsukuba, 305-8577, Japan
[5]Department of Meteorology, University of Reading, Reading, RG6 6ET, UK

*Correspondence to*: Yuya Takane (takane.yuya@nies.go.jp)

**Abstract.** We developed and released the single-layer urban canopy model (SLUCM) coupled with building energy model (BEM) v2.0, a single-layer urban canopy and building energy model capable of accurately simulating urban climates and electricity consumption (EC) across broad areas with substantially lower computational cost than conventional models. The previous version (v1.0) was a simplified model that set boundary conditions for wall and roof temperatures equal to the heating and air conditioning (HAC) setpoint. This prevented the calculation of indoor temperatures ($T_{in}$) under natural ventilation conditions (i.e. without HAC), limiting its applicability to wider regions and scenarios. This simplification was also identified as a key factor in the overestimation of EC in office districts of Tokyo. To address these issues, this study introduced a new version of the model in which $T_{in}$ varies dynamically based on HAC usage, outdoor temperatures, and ventilation conditions. This enables $T_{in}$ to be calculated during natural ventilation, and was shown to yield results consistent with observations from residential buildings in London under free-running conditions. Additionally, the overestimation of EC in office districts of Tokyo was significantly reduced. This upgrade facilitates the assessment of climate change adaptation measures for both outdoor and indoor environments. It enables an explicit simulation of the interactions between indoor and outdoor climates and human activities, including the consequent increase in outdoor temperatures due to anthropogenic heat emissions. The model is compatible with standard geographical datasets and existing WRF land-surface and urban physics options. SLUCM+BEM v2.0 is released both as an online WRF-coupled implementation and as a standalone version.

## 1 Introduction

Urban areas experience more pronounced warming, and consequently increased hazards, compared to suburban areas due to the combined effects of global climate change and local urban warming (IPCC 2023). Furthermore, the combination of high exposure (population density) and vulnerability (ageing populations and lack of access to cooling infrastructure) makes urban areas extremely high-risk environments in the modern era (IPCC 2023). A prime example of this heightened risk was the

https://doi.org/10.5194/egusphere-2026-1307
Preprint. Discussion started: 1 April 2026


European heatwave of 2003. In cities where air conditioning (AC) was not widespread, the heatwave resulted in an additional 70,000 deaths (Robine et al., 2008). Hokkaido, the northernmost island of Japan, where AC is less common, outdoor temperatures approaching 40°C have recently been observed, raising heat-related health concerns. However, heat-related mortality is not confined to places with low AC prevalence; it also occurs in regions where AC is widely adopted. For example, on Japan's main island (excluding Hokkaido and parts of Tohoku), where AC penetration currently exceeds 90%, a typhoon that hit the Tokyo metropolitan area (TMA) in 2019 caused localised power outages. In affected neighbourhoods, the resulting inability to operate AC during the subsequent heatwave was associated with a doubling of the risk of heatstroke-related emergency hospitalisations (Yamasaki et al. 2024). Furthermore, even in the absence of such compound events, many older adults limit their AC use during heatwaves, with important health consequences (Hampo et al. 2024).

With increasingly evident climate change, AC is a crucial adaptation measure to mitigate vulnerability (e.g., Chua et al. 2023) but requires energy for operation. AC driven electricity consumption (EC) use is projected to increase with climate change (IEA, 2018; Takane et al., 2023). While AC provides indoor comfort, it also contributes to local outdoor warming (increasing hazards) by expelling the energy used and the accumulated indoor cooling load as anthropogenic heat ($Q_F$) from the outdoor unit ($Q_{FB}$) (Ohashi et al. 2007; Salamanca et al. 2014; Takane et al. 2017), leading to further increases in $Q_{FB}$ and local warming (Takane et al. 2019; Kikegawa et al. 2022; Li et al. 2024a). Nevertheless, reports indicate the health benefits from using AC substantially outweigh the harms associated with $Q_{FB}$-driven local outdoor warming (Chua et al., 2023), and ACs remain a crucial adaptation to rising temperatures. However, the energy mix supplying electricity for AC operation may also contribute to greenhouse-gas emissions and hence global warming (Li et al. 2024a). AC deployment therefore entails a trade-off between near-term health protection and long-term environmental impacts.

Urban climate and building energy modelling (Table 1) has aided quantitative understanding of this trade-off through quantifying the feedback between AC use and warming, facilitating urban climate and energy processes prediction, and evaluation of climate change adaptation and mitigation strategies. The first of this type in meteorology and climate fields, CM-BEM (Kikegawa et al., 2003) primarily focuses on regional-scale assessments for specific urban areas within its metropolitan region. Subsequently other similar model were developed, including BEP+BEM (Building Effect Parameterization+Building Energy Model) (Salamanca et al. 2010) - an official integration into Weather Research and Forecasting model (Skamarock et al., 2021), BEM-TEB (BEM-Town Energy Budget) (Bueno et al. 2012), UT&C-BEM (Urban Tethys-Chloris-BEM) (Meili et al. 2020; 2025), and at the global scale CLMU (Community Land Model Urban) (Oleson et al. 2008; Oleson and Feddema 2020). Whereas all the Table 1 models are land surface models designed for, or capable of, coupling with meteorological and climate models, but does not include detailed standalone building energy models (e.g., EnergyPlus [Crawley et al. 2001]; DASH [Capel-Timms et al. 2020]; BIPV Window [Chen et al. 2021]) primarily designed for other purposes.

Takane et al.'s (2024) SLUCM+BEM v1.0 (Table 1) was developed for coupling to regional and global climate models. The standalone version successfully reproduced observed energy and radiation fluxes (upward short wave and long wave radiations

https://doi.org/10.5194/egusphere-2026-1307
Preprint. Discussion started: 1 April 2026


[Sup and Lup], sensible and latent heat fluxes [$Q_H$, and $Q_E$], net radiation (Q*), and storage flux [Q*-($Q_H$+$Q_E$)]) at Yoyogi, Tokyo (Hirano et al. 2015; Sugawara et al. 2021) over July–August 2018 and Jan–February 2017 (Takane et al. 2024). When coupled with WRF, SLUCM+BEM v1.0 also captures, some of the observed spatial patterns in outdoor 2-m air temperature and EC across the TMA (Takane et al. 2024). SLUCM+BEM v1.0 assumes that the indoor wall and ceiling temperatures (i.e. the boundary conditions) are equal to the heating and air conditioning (HAC) setpoint (see Fig. 1a, top). This assumption has the following drawbacks:

1) EC was qualitatively overestimated (Oleson and Feddema 2020; Takane et al. 2024)
2) The framework could not represent periods when AC is not operating, precluding simulation under naturally ventilated conditions

Issue 1 likely arises from the aforementioned assumption (Oleson and Feddema, 2020). It is improbable that indoor wall or ceiling surface temperatures equal the HAC setpoint throughout the summer and winter seasons. Specifically, during the cooling season (summer), the outdoor temperature is higher than the indoor temperature ($T_{in}$) for most periods. Consequently, heat flows from outdoors to indoors, leading to an indoor wall surface temperature > $T_{in}$. In reality, AC is used to bring the $T_{in}$ closer to the setpoint. However, v1.0 assumes the setpoint is the higher temperature of the interior wall surface, leading to an overestimation of EC. The opposite situation occurs in winter (heating season).

Issue 2 implies that the model cannot calculate the $T_{in}$ during periods without HAC, i.e. under natural ventilation conditions. This suggests that v1.0 is not readily applicable to cities where HAC penetration and/or usage is low, or to seasons and scenarios in which HAC is not required. Furthermore, as HAC represents a key climate adaptation measure, this limitation prevents evaluation of HAC impacts on indoor and outdoor thermal environments, energy use and health. Given that a substantial share of heat-related mortality occurs indoors, the inability to model indoor conditions without HAC is a significant shortcoming.

To address these issues, this study introduces SLUCM+BEM v2.0, which dynamically simulates $T_{in}$. We evaluated the resulting $T_{in}$ against observational data. Although several existing urban canopy–building energy modelling frameworks already compute $T_{in}$(Table 1; Lipson *et al.*, 2023), few studies explicitly validate simulated $T_{in}$ with measurements. Providing such a validation is therefore a key contribution of this work, and the evaluation protocol presented here should be transferable to other models. Furthermore, we compared the v2.0 results with those of v1.0 prior to its introduction, to demonstrate the contribution of $T_{in}$ modelling to the reproducibility of EC. The impact of $T_{in}$ modelling on EC has already been qualitatively recognised in the pioneering study by Oleson and Feddema (2020). However, quantitative evidence remains scarce, largely because high-resolution (spatially and temporally resolved) EC observations across urban areas are rarely available. This study benefits from extensive EC measurement data collected by the authors (Nakakajima et al., 2022; Takane et al., 2023a; 2023b), which also provide an important reference for similar models.

https://doi.org/10.5194/egusphere-2026-1307
Preprint. Discussion started: 1 April 2026


To position SLUCM+BEM v2.0 more explicitly relative to the previously published v1.0, the advances presented here can be separated into methodological developments and their demonstrated consequences. The methodological developments of v2.0 are twofold: first, the fixed HAC-setpoint boundary condition used in v1.0 was replaced by a prognostic $T_{in}$ formulation; second, ventilation processes were introduced so that $T_{in}$ can be simulated under both HAC and free-running conditions. These developments directly address the two principal limitations of v1.0, namely the likely bias in EC associated with the fixed boundary-condition simplification and the inability to simulate indoor conditions when HAC is not operating. The consequences of these developments are then demonstrated in this study through the validation of free-running $T_{in}$ against observations in London and the improved reproduction of EC in Tokyo relative to v1.0. Thus, v2.0 is not merely a parameter update, but a substantive extension of the SLUCM+BEM framework. We have summarised the advances in Table 2.

SLUCM+BEM v2.0 can evaluate the effectiveness of climate change adaptation and mitigation measures in urban environments, considering not only outdoor temperatures (as many urban canopy models do) but also $T_{in}$ and EC. Furthermore, it is designed for global city applications at relatively low computational cost (see Section 4). This paper presents the model development and validation that underpin future multi-city assessments and projections.

Furthermore, SLUCM+BEM v2.0 is coupled to WRF, allowing it to leverage recent additions to WRF-Urban that integrate external datasets, including spatially distributed urban parameters (Varquez et al., 2021; Khanh et al., 2023) and local climate zones (LCZs) (Demuzere et al., 2022). Given SLUCM's extensive global user base, upgrading this framework is particularly impactful, and SLUCM+BEM is expected to become an attractive option for many WRF users.

**Table 1: Description of urban canopy and building energy parameterisations for reginal and global climate models.**

| | SLUCM | SLUCM+BEM v1.0[1] | **SLUCM+BEM v2.0** | BEP+BEM[2] | CM-BEM[3] | CLMU[4, 5] | BEM-TEB[6] | UT&C-BEM[7] |
|---|---|---|---|---|---|---|---|---|
| $Q_F$ from buildings | Prescribed | Dynamic | **Dynamic** | Dynamic | Dynamic | Dynamic | Dynamic | Dynamic |
| $Q_F$ from traffic | Prescribed | Prescribed | **Prescribed** | – | Prescribed | Prescribed | Prescribed | – |
| Internal heat gain | – | Input | **Input** | Input | Input | – | Input | Input |
| $EC_{HAC}$ | – | Dynamic | **Dynamic** | Dynamic | Dynamic | Dynamic | Dynamic | Dynamic |
| Partial AC | – | Implemented | **Implemented** | Implemented | Implemented | Implemented | – | Implemented |
| COP | – | Dynamic | **Dynamic** | Constant | Dynamic | Constant | Dynamic | Constant |
| Cooling tower | – | Implemented | **Implemented** | – | Implemented | – | – | – |
| Windows | – | – | **–** | Implemented | Implemented | – | Implemented | Implemented |
| Ventilation | – | – | **Implemented** | Implemented | Implemented | Implemented | Implemented | Implemented |
| Indoor temperature | – | Prescribed | **Dynamic** | Dynamic | Dynamic | Dynamic | Dynamic | Dynamic |
| Weekday–weekend difference | – | – | **–** | – | Implemented | – | – | – |
| Coupled atmospheric model | WRF | WRF | **WRF** | WRF | WRF | CESM | WRF | – |
| Computational cost [-] *.[8] | 1.0 | 1.0 | **1.0** | 2.3 | 1.7 | – | 0.8 | – |

AC, air conditioning; BEM, building energy model, BEP, building effect parameterisation; CLMU, community land model–urban; CM, canopy model; COP, coefficient of performance; EC, electricity consumption; $Q_F$, anthropogenic heat, SLUCM, single-layer urban canopy model; TEB, town energy balance; UT&C, Urban Tethys-Chloris.

https://doi.org/10.5194/egusphere-2026-1307
Preprint. Discussion started: 1 April 2026


[1] Takane et al. (2024), [2] Salamanca et al. (2010), [3] Kikegawa et al. (2003), [4] Oleson and Feddema (2020), [5] Li et al. (2024b), [6] Bueno et al. (2012) , [7] Meili et al. (2020), [8]Kikegawa et al. (2025).

* Normalised computational time when simulating coupling with WRF by SLUCM

**Table 2: Direct comparison between SLUCM+BEM v1.0 and v2.0, highlighting the main limitations of v1.0, the substantive developments introduced in v2.0, and the evidence presented in this study.**

| Aspect | SLUCM+BEM v1.0 | Limitation in v1.0 | Substantive development in v2.0 | Evidence in this study |
|---|---|---|---|---|
| Indoor thermal representation | Boundary conditions for indoor wall and roof/ceiling temperatures were set equal to the HAC setpoint | Indoor surface temperatures were constrained unrealistically, which likely biased thermal loads and EC | The fixed HAC-setpoint boundary condition was replaced by a dynamic indoor temperature ($T_{in}$) formulation | Improved EC reproduction relative to v1.0 |
| Simulation when HAC is off | $T_{in}$ could not be calculated under free-running / natural-ventilation conditions | The model was not readily applicable to cities, seasons, or scenarios with low or no HAC use | $T_{in}$ is now solved dynamically under both HAC and non-HAC conditions | Free-running $T_{in}$ was evaluated against observations in London (MAE = 0.63–0.65°C) |
| Ventilation treatment | Ventilation was not explicitly represented in the indoor thermal-load calculation | Indoor heat exchange under natural ventilation was not captured | Ventilation processes were introduced into the indoor thermal-load calculation | This enables physically consistent free-running simulations and contributes to improved EC estimates |
| EC bias in Tokyo office districts | EC was qualitatively overestimated (MAE = 3.5 W floor-m$^{-2}$ in summer; 2.1 W floor-m$^{-2}$ in winter) | Confidence in building-energy application at district scale was reduced | Dynamic $T_{in}$ modelling and ventilation treatment reduced the bias | MAE decreased to 1.7 W floor-m$^{-2}$ in summer and 1.5 W floor-m$^{-2}$ in winter |
| Scope of applications | Mainly suitable for conditions with active HAC | Could not consistently assess indoor overheating, no-AC conditions, or outage-like scenarios together with outdoor feedbacks | Indoor and outdoor climates, EC, and anthropogenic heat can be evaluated consistently across AC-use scenarios | In the TMA no-AC case, daytime $Q_F$ decreased by ~40 W m$^{-2}$, outdoor temperature by ~0.2°C on average, while daytime $T_{in}$ increased by >3°C |
| Position relative to earlier SLUCM+BEM work | Low-cost SLUCM+BEM framework, but without prognostic $T_{in}$ | Limited applicability to broader adaptation assessments | Prognostic $T_{in}$ was added while retaining the SLUCM+BEM framework and broad-area applicability | v2.0 extends the model from outdoor/EC-focused applications to indoor–outdoor adaptation analyses |

Note: HAC, heating and air conditioning; $T_{in}$, indoor air temperature; EC, electricity consumption; $Q_F$, anthropogenic heat emission; MAE, mean absolute error; TMA, Tokyo metropolitan area.

# 2 Methods

## 2.1 Model development

### 2.1.1 SLUCM+BEM version 1.0

First, a brief overview of SLUCM+BEM v1.0 is provided, followed by a comparison with v2.0.

Figure 1a shows a conceptual diagram of SLUCM+BEM v1.0. In v1.0, $T_{in}$ was not modelled. Instead, the boundary conditions TBLEND and TRLEND for the walls and roof, respectively, as defined in the original SLUCM, were assumed to be the HAC

https://doi.org/10.5194/egusphere-2026-1307
Preprint. Discussion started: 1 April 2026


setpoint temperature and entered as fixed values (see Fig. 1a). Heat transfer through the walls and roof (HTRANS) was calculated using the following formula:

$$HTRANS = 2h\,AKSB\left(\frac{TBL(4) - TBLEND}{(\frac{DZB(4)}{2})}\right) + r\,AKSR\left(\frac{TRL(4) - TRLEND}{(\frac{DZR(4)}{2})}\right) \quad (1)$$

where the first and second terms on the right-hand side are conductive heat fluxes through walls and roofs, respectively; $h$ and $r$ are the normalised building height and roof width, respectively, as defined by Kusaka et al. (2001); *AKSB* and *AKSR* are the thermal conductivity of walls and roofs (W m$^{-1}$ K$^{-1}$), respectively; and *DZB* and *DZR* are the thickness of each layer of walls and roofs, respectively. Then, HTRANS was the first term on the right-hand side of the indoor sensible heat load ($H_{in}$) equation (see Fig. 1a, bottom; Equation 2):

$$H_{in} = HTRANS + A_f qE + A_f P \varphi_P q_{hs} \quad (2)$$

where the right-hand side shows each component of the $H_{in}$. The first term is the *HTRANS* estimated using Eq. (1). The second and third terms are the internal sensible heat generation by the equipment and occupants, respectively (always positive). In the terms, $A_f$ is the floor area (floor m$^{-2}$), $qE$ is the sensible heat gain from appliances per floor area (W floor m$^{-2}$), $P$ is the peak number of occupants per floor area (person floor-m$^{-2}$), $\varphi_P$ is the ratio of hourly occupants to $P$ (dimensionless), and $q_{hs}$ is the sensible heat generation from building occupants (W person$^{-1}$). For simplification, the model did not consider the transmission of solar insolation through windows or sensible heat exchange through ventilation.

From this $H_{in}$, the heating/cooling load $H_{out}$ processed by the HAC was calculated:

$$H_{out} = H_{in} \times (1 - a) \times b \times c. \quad (3)$$

where a, b and c are the ratio of abandoned houses/buildings to all houses/buildings (AB_BUILD_RATIO), the ratio of the air-conditioned floor area to the total floor area (AC_FLOOR_RATIO), and the ratio of the electric HAC usage for cooling or heating to all cooling or heating equipment (AC_USAGE_RATIO_CL and AC_USAGE_RATIO_HT for cooling and heating), respectively. The settings for these parameters are provided in Table 3.

Using $H_{out}$ (Eq. 3) and the coefficient of performance (*COP*) that was reproduced by Eq. (4) in Takane et al. (2024), $EC_{HAC}$ and the anthropogenic heat ($Q_F$) from buildings ($Q_{FB}$; positive in summer and negative in winter) was calculated at each time step as follows:

$$EC_{HAC} = \frac{|H_{out}|}{COP}. \quad (4)$$

https://doi.org/10.5194/egusphere-2026-1307
Preprint. Discussion started: 1 April 2026


$$Q_{FB} = H_{out} + E_{HAC} = \frac{COP + 1}{COP} H_{out}; during\ cooling\ operation\ (summer), \quad (5)$$

$$Q_{FB} = H_{out} - E_{HAC} = \frac{COP - 1}{COP} H_{out}; during\ heating\ operation\ (winter), \quad (6)$$

In the Northern Hemisphere, we assumed a cooling operation from June to September and a heating operation from November to March. In the Southern Hemisphere, these periods were reversed, with cooling assumed from November to March and heating from June to September. Alternative cooling and heating schedules could be prescribed using the outdoor air temperature simulated by SLUCM and WRF, rather than by calendar month. $Q_{FB}$ is added to $Q_F$ from traffic ($Q_{FT}$), which is input separately from URBPRAM.TBL and added to sensible heat flux ($Q_H$). It is then fed back to the atmosphere (see Fig. 1a, bottom). However, as mentioned in the Introduction, v1.0 had the following issues: (1) TBLEND and TRLEND were input as fixed values and assumed to represent the HAC setpoint temperature. Consequently, calculations were performed under the assumption that the $T_{in}$ was always equal to the AC setpoint temperature (TBLEND = TRLEND). Therefore, it was impossible to perform calculations considering situations where HAC was absent or not in use. This limitation meant that v1.0 could only be used in certain cities worldwide. (2) An overestimation of $EC_{HAC}$ remained, which was likely attributable to the limitation described in (1) (see Introduction for details).

https://doi.org/10.5194/egusphere-2026-1307
Preprint. Discussion started: 1 April 2026


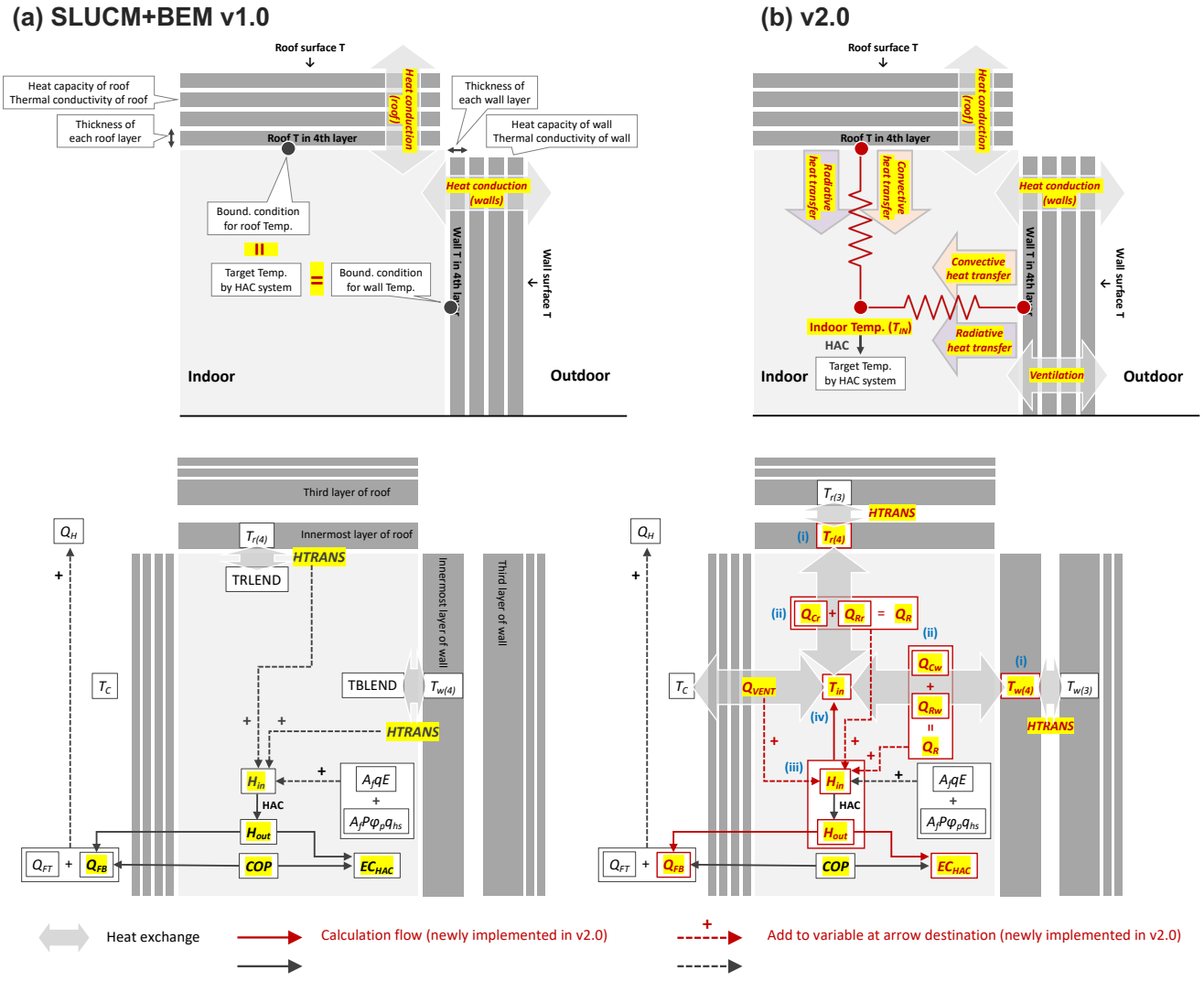


**Figure 1: Top: schematic of the energy budgets for an urban canopy layer that includes buildings. The single-layer urban canopy model (SLUCM) coupled with building energy model (BEM) version (a) 1.0 and (b) 2.0. Dark red and yellow highlighting indicate variables simulated by SLCUM+BEM. The text in the callouts indicates original or newly introduced inputs to the WRF parameter table URBNPRAM.TBL. Bottom: flow-chart of BEM related variables for SLUCM+BEM (a) v1.0 and (b) v2.0. Dark red and yellow highlighting indicate variables simulated by SLCUM+BEM v2.0. The blue numbers (i)–(iv) correspond to those in section 2.1.2.**

165

https://doi.org/10.5194/egusphere-2026-1307
Preprint. Discussion started: 1 April 2026


### 2.1.2 SLUCM+BEM version 2.0

This study proposes v2.0 to address the issues identified in v1.0. The most significant improvements are the modelling of $T_{in}$ and the introduction of a ventilation process that constitutes $H_{in}$ (see Fig. 1b). The specific calculation is as follows (corresponding to the blue numbers at the bottom of Fig. 1b):

(i) Calculate the innermost roof and floor temperatures.

(ii) Determine the heat exchange (convection and radiation) between the innermost ceiling/wall surface temperature and the $T_{in}$.

(iii) Update and add the indoor heat load (introduce the ventilation process).

(iv) Calculate the $T_{in}$ from the updated indoor heat load and that processed by the HAC system.

Regarding (i), the temperature of the innermost layer of the walls and roof is calculated as follows:

$$CAPR \cdot DZR(4)\frac{dTRL(4)}{dt} = -AKSR\left(\frac{TRL(3)-TRL(4)}{DZR(3)-DZR(4)}\right) - Q_{Cr} - Q_{Rr} \quad (7)$$

$$CAPB \cdot DZB(4)\frac{dTBL(4)}{dt} = -AKSB\left(\frac{TBL(3)-TBL(4)}{DZB(3)-DZB(4)}\right) - Q_{Cw} - Q_{Rw} \quad (8)$$

where *CAPR* and *CAPB* are the heat capacity of the roof and building wall (J m$^{-3}$ K$^{-1}$), respectively; $Q_{Cr}$, $Q_{Cw}$, $Q_{Rr}$ and $Q_{Rw}$ are the convective heat transfer from the roof and building wall, and the radiative heat transfer from the roof and the building wall (W m$^{-2}$), which are calculated by Eqs. (10)–(11) and (16)–(17), respectively.

Regarding (ii): The heat transfer is calculated using the formula derived from the difference between dTRL(4) and dTBL(4), as calculated above, and the $T_{in}$ value from the previous step, as described below. The total convective heat transfer from the interior wall and ceiling is described by the following formula:

$$Q_C = Q_{Cr} + Q_{Cw} \quad (9)$$

The respective convective heat transfer rates from the ceiling and interior wall are described by assuming natural convection over a vertical flat plate:

$$Q_{Cr} = h_C(TRL(4) - T_{in}) \quad (10)$$

$$Q_{Cw} = h_C(TBL(4) - T_{in}) \quad (11)$$

where $h_C$ is the conductivity of convective heat transfer (W m$^{-2}$ K$^{-1}$) estimated by:

https://doi.org/10.5194/egusphere-2026-1307
Preprint. Discussion started: 1 April 2026


$$h_C = \begin{cases} 0.56\frac{\lambda_a}{d_Z}(Gr\ Pr)^{0.25}, & 10^4 < Gr\ \mathrm{Pr} < 10^9 \\ 0.13\frac{\lambda_a}{d_Z}(Gr\ Pr)^{0.33}, & 10^9 < Gr\ \mathrm{Pr} < 10^{12} \end{cases} \quad (12)$$

$$G_r = \frac{2{d_z}^3 g|TBL(4) - T_{in}|}{\nu^2(TBL(4) + T_{in})} \quad (13)$$

$$P_r = \upsilon\frac{C_p\rho}{\lambda_a} \quad (14)$$

where $\lambda_a$ is the thermal conductivity of air (W m$^{-1}$ K$^{-1}$); $d_Z$ is the length scale (m) assuming the building height in this study; $G_r$ is the Grashof number (dimensionless); $P_r$ is the Prandtl number (dimensionless); $\nu$ is the dynamic viscosity of air (m$^2$ s$^{-1}$); and $g$ is acceleration due to gravity (m s$^{-2}$).

Similar to convection, the heat transport due to radiation is calculated using the following equation, as with CM–BEM (Kikegawa et al. 2003):

$$Q_R = Q_{Rr} + Q_{Rw} \quad (15)$$

$Q_{Rr}$ and $Q_{Rw}$ are estimated by:

$$Q_{Rr} = h_R(TRL(4) - T_{in}) \quad (16)$$

$$Q_{Rw} = h_R(TBL(4) - T_{in}) \quad (17)$$

where $h_R$ is the conductivity of radiative heat transfer (W m$^{-2}$ K$^{-1}$), estimated by:

$$h_R = 4\varepsilon_w\sigma{T_{in}}^3 \quad (18)$$

where $\varepsilon_w$ is the thermal conductivity of air (W m$^{-1}$ K$^{-1}$), and $\sigma$ is the dynamic viscosity of air (m$^2$ s$^{-1}$).

Regarding (iii), v2.0 incorporates the $Q_C$ and $Q_R$ values calculated above into $H_{in}$, whereas v1.0 incorporates them into HTRANS. Furthermore, the absence of a ventilation process was identified as a limitation of v1.0 (Takane et al., 2024). Consequently, heat exchange due to ventilation has been added. This is described below:

$$Q_{VENT} = C_p\rho V_a(T_c - T_{in}) \quad (19)$$

where $T_C$ is the urban canopy outdoor temperature (K); $V_a$ is the air exchange between indoor and outdoor per floor (m$^3$ s$^{-1}$ m$^{-2}$) calculated by:

$$V_a = \frac{(VENT\_RATE \cdot total\_floor\_area)}{3{,}600} \quad (20)$$

https://doi.org/10.5194/egusphere-2026-1307
Preprint. Discussion started: 1 April 2026


where VENT_RATE is the ventilation rate (dimensionless) from the input file (URBPRAM.TBL) (Table 3). For residential buildings (both detached and multi-unit dwellings), we set VENT_RATE = 0.5 $h^{-1}$ (Table 3) consistent with the minimum continuous ventilation requirement for habitable rooms in dwellings stipulated in the Japanese Building Standards Act sick-house countermeasure guidance (Ministry of Land, Infrastructure, Transport and Tourism of Japan [MLIT] https://www.mlit.go.jp/jutakukentiku/build/sickhouse.files/setumeishiryou.pdf). For business and commercial buildings, the value VENT_RATE = 1.7 $h^{-1}$ (Table 3) follows the standard office-building setting used in the original CM–BEM framework. In Kikegawa et al. (2003), the outdoor air introduction rate for a typical office building is specified as 5.0 $m^3\ m^{-2}\ h^{-1}$. Assuming a representative floor-to-ceiling height of 3.0 m in the model, this corresponds to an air-change rate of 5.0/3.0 = 1.67 $h^{-1}$, rounded to 1.7 $h^{-1}$.

As a result, $H_{in}$ in v2.0 becomes:

$$H_{in} = Q_C + Q_R + Q_{VENT} + A_f qE + A_f P \varphi_P q_{hs}. \quad (21)$$

Regarding (iv), the indoor heating/cooling load processed by HAC is calculated using Eq. (3), as in v1.0. The indoor temperature ($T_{in}$) is then determined as follows:

$$Q_B \frac{dT_{in}}{dt} = H_{in} - H_{out}. \quad (22)$$

where $Q_B$ is the total indoor heat capacity (J $K^{-1}$).

The following parameters have been added with the update to SLUCM+BEM v2.0:

- 'SBEMOPTION': 0 = Use SLUCM; 1 = Use SLUCM+BEM v2.0
- 'AH_TRAFFIC' (W $m^{-2}$) = Anthropogenic heat ($Q_F$) from traffic ($Q_{FT}$) input when 'SBEMOPTION' = 1
- 'TARGTEMP' (K) = Setpoint temperature for HAC system Use the parameters introduced for BEP+BEM
- "VENT_RATE" (–): Ventilation rate

Enter these parameters into the URBPRAM.TBL or URBPRAM_LCZ.TBL input table (see Table 3).

The $H_{out}$ and COP are calculated using the same formula as v1.0, and $Q_{FB}$ is fed back to the atmosphere of WRF through $Q_H$ (Fig. 1b, bottom). Note that, in the current version of SLUCM+BEM v2.0, $Q_F$ does not directly impact the temperature of the air in the canyon ($T_C$), as reported by Li et al. (2024c).

https://doi.org/10.5194/egusphere-2026-1307
Preprint. Discussion started: 1 April 2026


### 2.2 Model settings

This study involves conducting online coupled simulations with WRF in the TMA in Japan, alongside standalone offline SLUCM+BEM simulations in London in the UK.

#### 2.2.1 Online simulation for the Tokyo Metropolitan Area

The online simulation settings used in this study are identical to those in v1.0 (Takane et al., 2024). Only an overview is provided here. For more information, please refer to Takane et al. (2024).

The present study used Advanced Research WRF (ARW) ver. 4.3.2 (Skamarock et al., 2021), coupled online with SLUCM+BEM. Figure 2 shows the finest model domain (d03), containing 251 grid points in the x and y directions, covering the TMA, which was the focus of our study. Domains 1 (d01) and 2 (d02) cover all of Japan and the central area of Japan, respectively. We set the horizontal grid spacing to 25, 5, and 1 km for domains d01, d02, and d03, respectively. The model top was 50 hPa, with 37 vertical sigma levels. In this simulation, the initial and boundary conditions were derived from the National Centres for Environmental Prediction Global Tropospheric Final Analysis (NCEP–FNL) from the Global Data Assimilation System with 0.25° horizontal grid spacing (GDAS, 2015), and Group for High-Resolution Sea Surface Temperature (GHRSST) Level 4 data with 1-km horizontal grid spacing (Chao et al., 2009).

The following schemes were used in the simulation: the updated Rapid Radiation Transfer Model (RRTMG) short- and long-wave radiation schemes (Iacono et al., 2008), Morrison 2-moment cloud microphysics scheme (Morrison et al., 2009), Mellor–Yamada–Janjic atmospheric boundary-layer scheme (Mellor & Yamada, 1982; Janjic, 1994; 2002), Noah land surface model (Chen & Dudhia, 2001), and SLUCM (Kusaka et al., 2001; Kusaka & Kimura, 2004) or SLUCM+BEM v2.0 as proposed in this study.

The urban grids were classified into three categories (C, Rm, and Rd) based on the dominant building type, as with Takane et al. (2022; 2024) and Nakajima et al. (2021; 2023). This is shown in Fig. 2a.

The simulation was conducted from 09:00 JST (00:00 UTC = 09:00 JST) on 25 June to 09:00 JST on 31 August 2018 for the summer case, and from 25 December 2016 to 28 February 2017 for the winter case. For each case, the first 5 days were discarded as the model spin-up period. In Tokyo, the HAC is generally used only in summer and winter (not in spring and autumn) (Takane et al., 2017). The summer and winter of 2017 and 2018 were selected because measurements of EC were available (Nakajima et al., 2022), and there were more clear-sky days in these than in other years.

We ran three simulation types: the original SLUCM with AHOPTION = 1, SLUCM+BEM v1.0 with AHOPTION = 2 and v2.0 with SBEMOPTION = 1. The main parameters entered for each simulation type are listed in Table 3. Note that

https://doi.org/10.5194/egusphere-2026-1307
Preprint. Discussion started: 1 April 2026


AHOPTION = 2 only works for v1.0. In v2.0, the role of AHOPTION = 2 has changed to SBEMOPTION = 1 to avoid any misunderstandings. Another new option, AH_TRAFFIC, has also been added in v2.0 as described in section 2.1.2.

In the SLUCM case, $Q_F$ was an aggregate of all sources, with a maximum value (AH) and temporal variation (AHDIUPRF) for each urban category. In this study, AH and AHDIUPRF were obtained from the sum of $Q_{FB}$ calculated by CM-BEM for each grid and the separately input $Q_F$ from traffic for each building category (Nakajima et al., 2023). In the SLUCM+BEM case, $Q_{FB}$ is the simulated variable, such that $Q_F$ from traffic was given as AH & AHDIUPRF for v1.0, and AH_TRAFFIC & AHDIUPRF for v2.0 was the temporal pattern of $Q_F$ from traffic, in accordance with Nakajima et al. (2023). The ability to input $Q_F$ from traffic in this manner is a notable advantage of SLUCM+BEM over BEP+BEM (Table 1).

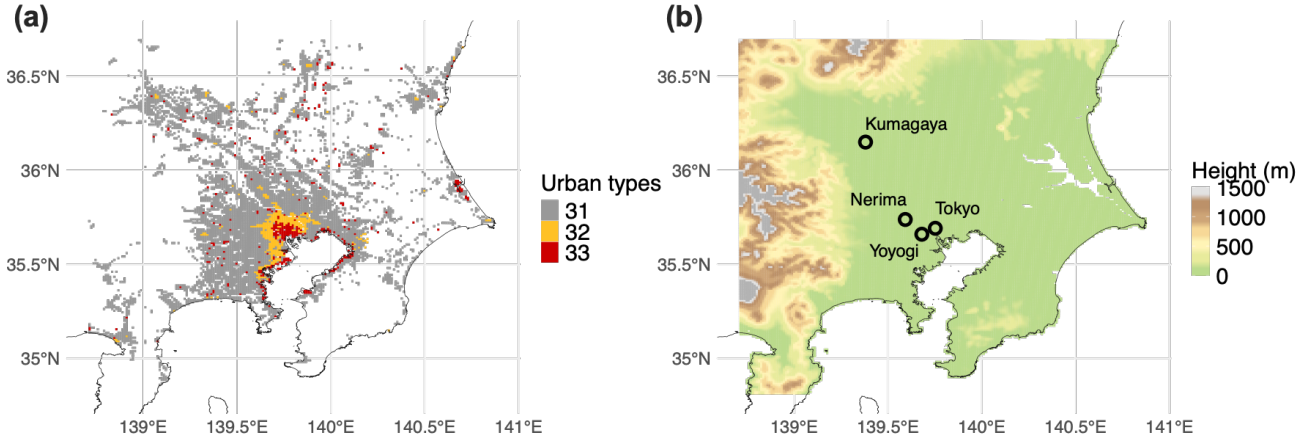


**Figure 2: Study area of the online simulation. (a) Distribution of three building use categories: residential area with detached dwellings (low-density residential, 31 [grey]), residential area with multi-unit dwellings (high-density residential, 32 [yellow]), and business and commercial buildings (commercial, 33 [red]) in the Tokyo metropolitan area (TMA). (b) Terrain height within the study area. Open circles indicate observation sites at Nerima, Kumagaya, and Yoyogi in Tokyo.**

**Table 3: Parameter settings for the SLUCM and SLUCM+BEM models (v1.0 and v2.0). The cooling and heating seasons (summer and winter) ran from 25 June to 31 August 2018, and from 25 December 2016 to 28 February 2017, respectively. The urban categories are: 1 low-density residential (Rd), 2 high-density residential (Rd), and 3 commercial (BC).**

| Parameter (units) [cases] | SLUCM | SLUCM+BEM v1.0 | SLUCM+BEM v2.0 |
|---|---|---|---|
| Season | Cooling, heating | | |
| ZR (m)<br>[Urban category = 1, 2, 3] | 7.4, 10.6, 15.2 | | |
| FRC_URB (–)<br>[Urban category = 1, 2, 3] | 0.7, 0.9, 0.9 | | |
| AHOPTION | 1 | 2 | 1 |

https://doi.org/10.5194/egusphere-2026-1307
Preprint. Discussion started: 1 April 2026


| | | | | | | |
|---|---|---|---|---|---|---|
| SBEMOPTION ** | 0 | | – | | 1 | |
| AH (W m$^{-2}$)<br>[Urban category = 1, 2, 3] | 38.8, 52.8, 141.5 in summer<br>19.4, 26.4, 70.7 in winter<br>(from all sources, including buildings and traffic) | | 3.3, 7.4, 10.8 (from traffic only) | | – | |
| AH_TRAFFIC (W m$^{-2}$)<br>[Urban category = 1, 2, 3] ** | – | | – | | 3.3, 7.4, 10.8 | |
| AHDIUPRF (–)<br>[Local time = hours 1–24] | 0.467 0.370 0.323 0.319 0.366 0.485 0.620 0.718 0.831 0.881 0.913 0.870 0.931 0.982 1.000 0.997 0.957 0.906 0.851 0.804 0.767 0.681 0.660 0.520 | | | | | |
| BOUNDR, BOUNDNB, BOUNDG (BOUND*) | 2 | | | | | |
| DDZR (m) [Layer = 1, 2, 3, 4] | 0.08, 0.08, 0.08, 0.08 | | | | | |
| DDZB (m) [Layer = 1, 2, 3, 4] | 0.06, 0.06, 0.06, 0.06 | | | | | |
| CAPR (J m$^{-3}$ K$^{-1}$)<br>[Urban category = 1, 2, 3] | $0.4521 \times 10^6$, $1.588 \times 10^6$, $1.298 \times 10^6$ | | | | | |
| CAPB (J m$^{-3}$ K$^{-1}$)<br>[Urban category = 1, 2, 3] | $0.674 \times 10^6$, $1.702 \times 10^6$, $1.598 \times 10^6$ | | | | | |
| AKSR (W m$^{-1}$ K$^{-1}$)<br>[Urban category = 1, 2, 3] | 0.071, 0.192, 0.094 | | | | | |
| AKSB (W m$^{-1}$ K$^{-1}$)<br>[Urban category = 1, 2, 3] | 0.094, 0.276 0.217, | | | | | |
| TRLEND (K)<br>[Urban category = 1, 2, 3] | 300, 304, 304 for cooling | 298.15, 290.15, 290.15 for heating | 300, 304, 304 for cooling | 298.15, 290.15, 290.15 for heating | 301, 301, 300 for cooling | 295.15, 295.15, 295.15 for heating |
| TBLEND (K)<br>[Urban category = 1, 2, 3] | 300, 304, 304 for cooling | 298.15, 290.15, 290.15 for heating | 300, 304, 304 for cooling | 298.15, 290.15, 290.15 for heating | 301, 301, 300 for cooling | 295.15, 295.15, 295.15 for heating |
| TARGTEMP (K) [Urban category = 1, 2, 3] ** | – | – | – | – | 301, 301, 300 for cooling | 295.15, 295.15, 295.15 for heating |
| HSEQUIP_SCALE_FACTOR (W floor-m$^{-2}$)<br>[Urban category = 1, 2, 3] | – | | 6.27, 6.84, 9.2 | | | |
| HSEQUIP (–)<br>[Local time = hours 1–24] | – | | 0.76, 0.72, 0.71, 0.71, 0.72, 0.72, 0.76, 0.80, 0.86, 0.90, 0.91, 0.92, 0.91, 0.93, 0.93, 0.93, 0.96, 0.99, 1.00, 0.98, 0.94, 0.90, 0.85, 0.81 | | | |
| AB_BUILD_RATIO (–)<br>[Urban category = 1, 2, 3] * | – | | 0.136, 0.136, 0.136 | | | |
| AC_FLOOR_RATIO (–)<br>[Urban category =1, 2, 3],<br>[Local time = hours 1–24] * | – | | Urban category 1:<br>0.38, 0.35, 0.34, 0.32, 0.30, 0.28, 0.26, 0.23, 0.21, 0.17, 0.17, 0.17, 0.17, 0.16, 0.16, 0.16, 0.16, 0.18, 0.20, 0.23, 0.29, 0.34, 0.37, 0.40 for cooling<br>0.537, 0.510, 0.470, 0.457, 0.430, 0.403, 0.376, 0.349, 0.309, 0.282, 0.228, 0.228, 0.228, 0.228, 0.215, 0.215, 0.215, 0.215, 0.242, 0.269, 0.309, 0.389, 0.457, 0.497 for heating<br>Set to be 0.0 for 24 hours in case of No-HAC<br>Urban category 2: | | | |

https://doi.org/10.5194/egusphere-2026-1307
Preprint. Discussion started: 1 April 2026


| | | | |
|---|---|---|---|
| | | 0.45, 0.40, 0.35, 0.33, 0.32, 0.31, 0.31, 0.31, 0.32, 0.33, 0.34, 0.34, 0.34, 0.34, 0.34, 0.34, 0.34, 0.35, 0.37, 0.39, 0.41, 0.42, 0.44, 0.45 for cooling<br>0.604, 0.604, 0.537, 0.470, 0.443, 0.430, 0.416, 0.416, 0.416, 0.430, 0.443, 0.457, 0.457, 0.457, 0.457, 0.457, 0.457, 0.457, 0.470, 0.497, 0.524, 0.551, 0.564, 0.591 for heating<br>Set to be 0.0 for 24 hours in case of No-HAC<br><br>Urban category 3:<br>0.20, 0.19, 0.19, 0.18, 0.18, 0.18, 0.25, 0.37, 0.48, 0.56, 0.59, 0.62, 0.62, 0.62, 0.62, 0.62, 0.62, 0.62, 0.55, 0.50, 0.44, 0.35, 0.24 for cooling<br>0.322, 0.269, 0.255, 0.255, 0.242, 0.242, 0.242, 0.336, 0.497, 0.645, 0.752, 0.792, 0.833, 0.833, 0.833, 0.833, 0.833, 0.833, 0.833, 0.833, 0.739, 0.671, 0.591, 0.470 for heating<br>Set to be 0.0 for 24 hours in case of No-HAC | |
| AC_USAGE_RATIO_CL (–) [Urban category = 1, 2, 3] * | – | 1, 1, 1 | |
| AC_USAGE_RATIO_HT (–) [Urban category = 1, 2, 3] * | – | 0.6, 0.6, 0.6 | |
| COPOPTION * | – | 1 | |
| COP [Urban category = 1, 2, 3] | – | 5.03, 5.03, 3.58 | |
| VENT_RATE (–) [Urban category = 1, 2, 3] ** | – | – | 0.5, 0.5, 1.7 for HAC use case<br>10.0, 10.0, 10.0 for no-HAC case |

AB_BUILD_RATIO, ratio of abandoned houses/buildings to all houses/buildings in a city block; AC_FLOOR_RATIO, ratio of air-conditioned floor area to total floor area; AC_USAGE_RATIO_CL, proportion of cooling AC usage; AC_USAGE_RATIO_HT, proportion of heating AC usage; AH, anthropogenic heat; AH_TRAFFIC, anthropogenic heat from traffic; AHDIUPRF, diurnal profile of anthropogenic heating; AHOPTION, anthropogenic heating option, where 0 = no anthropogenic heating and 1 = anthropogenic heating added to the sensible heat flux term; SBEMOPTION, SLUCM+BEM option, where 0 = SLUCM+BEM does not work, 1 = SLUCM+BEM works; AKSB, thermal conductivity of the building wall; AKSR, thermal conductivity of the roof; CAPB, heat capacity of the building wall; CAPR, heat capacity of the roof; COP, coefficient of performance; COPOPTION, a switch that determines whether COP is fixed or variable, where 0 = fixed COP and 1 = COP simulated by SLUCM+BEM; DDZB, thickness of each building wall layer; DDZR, thickness of each roof layer; FRC_URB, fraction of the urban landscape; HSEQUIP, proportional change in HSEQUIP_SCALE_FACTOR over time; HSEQUIP_SCALE_FACTOR, peak internal heat gain; TBLEND, lower boundary of the building wall temperature; TRLEND, lower boundary of the roof temperature; ZR, building height; TARGTEMP, target temperature by the HAC system; VENT_RATE, ventilation rate.

* Newly added to SLUCM+BEM v1.0; (–) dimensionless parameter.

** Newly added to SLUCM+BEM v2.0; (–) dimensionless parameter.

### 2.2.2 Offline simulation for Southwark, London

The SLUCM+BEM models were run in offline and online modes, coupled with WRF. In offline mode, SLUCM+BEM and Noah-LSM (Chen & Dudhia, 2001) were coupled with a mosaic of natural vegetation and urban tiles in accordance with the WRF online land surface processes. Forcing data were taken from the nearest grid value in the Southwark area of London from the ERA5 reanalysis (Hersbach et al., 2020), and the simulated results from SLUCM+BEM were compared with $T_{in}$ measured in the same area.

https://doi.org/10.5194/egusphere-2026-1307
Preprint. Discussion started: 1 April 2026


To verify the accuracy of the $T_{in}$ reproduction modelled by SLUCM+BEM v2.0, we used $T_{in}$ data collected in the Southwark area of London (see Fig. 3) (Zhao et al., 2023; Sun et al., 2025). London was chosen as the location for the temperature data because AC is not yet widespread in residential areas of London (Li et al., 2024), and even in homes with AC, the summer climate is not hot enough to warrant frequent use of AC. Therefore, $T_{in}$ values measured in this location are likely to be representative of natural ventilation conditions, making them suitable for verifying the $T_{in}$ modelled by SLUCM+BEM v2.0. Conversely, AC is widespread in Tokyo residences, and summer temperatures are high enough for constant AC use. Consequently, the measured $T_{in}$ at this location naturally approaches the AC setpoint temperature. Because SLUCM+BEM v2.0 is designed to approach $T_{in}$ at the setpoint when AC is operated (Equation 22), the model-calculated $T_{in}$ should naturally approach the measured setpoint temperature. Verifying this $T_{in}$ has limited significance. However, verifying the EC when the $T_{in}$ is brought close to the AC setpoint during operation is considerably more meaningful. This will be addressed as a separate verification in Section 3.2.

The simulation ran from 00:00 UTC on 1 July to 09:00 JST on 1 October 2023. The first 5 days were discarded as the model spin-up period. Even in summer, AC is generally not used in London. Therefore, the AC_FLOOR_RATIO (Table 3) was set to 0 for all time periods, assuming no AC was used. Furthermore, as $T_{in}$ data are available for both apartment (flat-type) buildings and detached houses, two simulations were performed with modified parameters for each building type, and the results were compared with the corresponding observed data. These parameters (including the thickness, thermal conductivity, heat capacity, albedo and emissivity of roofs and walls) were based on previous studies conducted in London (Loridan et al., 2013; Tsiringakis et al., 2019, 2020; Brousse et al., 2023).

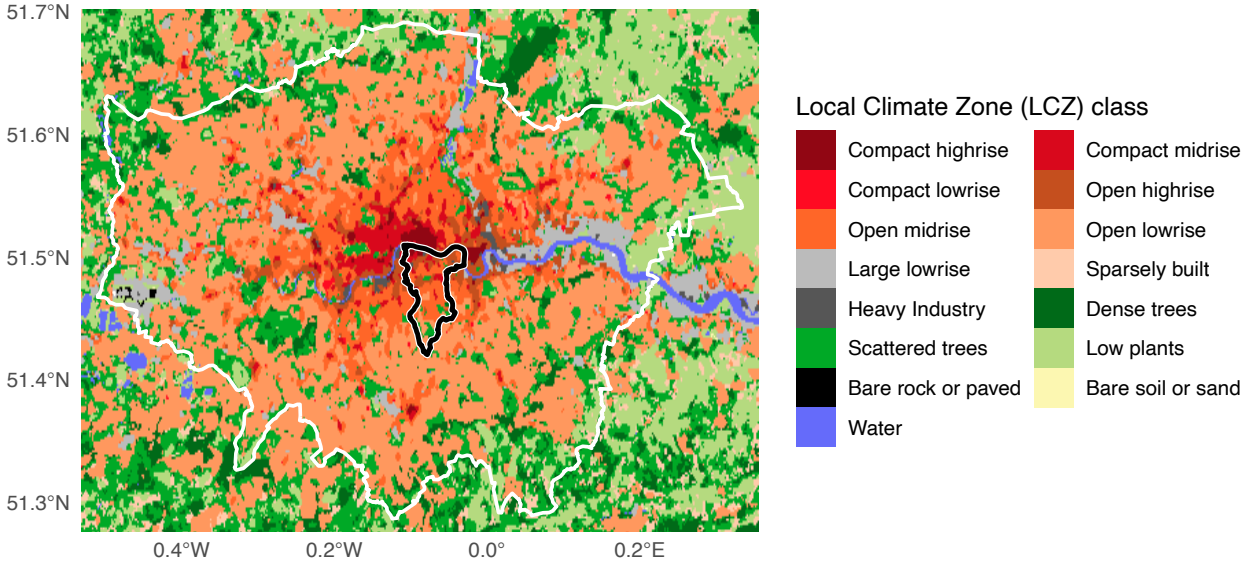

https://doi.org/10.5194/egusphere-2026-1307
Preprint. Discussion started: 1 April 2026


**Figure 3: Study area of the offline simulation. Distribution of local climate zone (LCZ) in Greater London. White and black lines indicate the boundaries of Greater London and Southwark, respectively.**

### 2.3 Metrix of verification

Section 3 presents an accuracy verification of SLUCM+BEM v2.0. The evaluation metrics used are mean bias error (MBE), mean absolute error (MAE), and root mean square error (RMSE). These are defined as follows:

$$MBE = \frac{1}{n}\sum_{i}^{n}(M_i - O_i) \quad (23)$$

$$MAE = \frac{1}{n}\sum_{i}^{n}|M_i - O_i| \quad (24)$$

$$RMSE = \sqrt{\frac{1}{n}\sum_{i}^{n}(M_i - O_i)^2} \quad (25)$$

where $n$ shows sample number (hour); and $M_i$ and $O_i$ represent the simulated and observed values in $i$, respectively.

## 3 Results

### 3.1 Indoor temperature ($T_{in}$)

Figure 4a shows measurements of $T_{in}$ in flats in the Southwark area of London from late July to September 2023. The grey lines indicate temperature values measured in each individual flat, while the black dotted line shows their average. Two principal features are evident in these observed data. First, there was significant variation in the measured $T_{in}$ among all flats, with a range of approximately 4–5°C between the maximum and minimum values. This substantial variation was likely due to human activity within each flat, particularly the extent of ventilation associated with opening and closing windows (Sun et al., 2025). Second, the average values show diurnal variations. These average values also fluctuated over periods of approximately 1 week. Specifically, from late July to early August, $T_{in}$ gradually decreased from around 24°C to 22°C. It then increased until 11 August, stabilising at 24–25°C until 25 August. From 25 to 31 August, it then decreased daily to around 22°C. It then increased daily until 10 September, reaching an average of around 28°C on that date. Sun et al. (2025) refer to this relatively warm period as a "mini-heatwave". $T_{in}$ then declined gradually. These fluctuations over days to weeks, along with diurnal variations, corresponded to changes in the outdoor temperature associated with changes in the daily weather and diurnal cycle. These $T_{in}$ characteristics were observed in both flats and detached houses within the same area (Fig. 4b).

https://doi.org/10.5194/egusphere-2026-1307
Preprint. Discussion started: 1 April 2026


SLUCM+BEM v2.0 was used to reproduce the temperature patterns described above. However, given the significant variability in the measurements, which were primarily due to differences in human activities such as window ventilation, the simulation did not attempt to replicate the temperature profile of each individual dwelling (grey lines). Instead, the focus was on whether SLUCM+BEM v2.0 could reproduce the range of this variability and the average value (black circles). This strategy aligns with SLUCM+BEM v2.0's design philosophy, as it is fundamentally an urban canopy model aimed at reproducing grid-average values rather than modelling individual buildings. Consequently, the SLUCM+BEM v2.0 reproduction experiment involved making calculations for multiple cases in which the ventilation rate (see Equation 16) varied from a minimum of 0 to a maximum of 10. A ventilation rate of 0 represents windows being completely closed, with no ventilation (evaluated as vent-0), while a rate of 10 (vent-10) simulates windows being frequently open. Altering the ventilation rate changes the components of the building's internal heat load, $Q_{VENT}$ (Equation 19) and $H_{in}$ (Equation 21), thereby altering the $T_{in}$ (Equation 22).

The red line in Fig. 4 shows the results of the SLUCM+BEM v2.0 experiments. The line indicating the highest $T_{in}$ corresponds to vent-0, while the dotted line showing the lowest temperature corresponds to vent-10. The figure shows that increased ventilation led to greater heat exchange with the outside air, causing $T_{in}$ to decrease. The uncertainty in $T_{in}$ due to the ventilation rate was approximately 3–7°C, which broadly covers the observed variation in the earlier measured values. This is a crucial point for this experiments because it supports the idea that the observed variability in $T_{in}$ stems from human activity, i.e. window opening. Furthermore, the thick red line shows the average values from several experiments with altered ventilation rates. Comparing this average with the observed average revealed that the model generally captured the observed daily and multi-day to weekly $T_{in}$ fluctuations mentioned earlier. Restricting the comparison to the period 2 August–13 September (selected by Sun et al., 2025) yielded very low bias metrics for flats: MBE of 0.00°C, MAE of 0.63°C and RSME of 0.67°C. Similar values were observed for detached houses (MBE: -0.16°C; MAE: 0.65°C; RSME: 0.69°C). Thus, SLUCM+BEM v2.0 broadly reproduced the range of variation and average values of $T_{in}$ under the observed natural ventilation conditions, together with their diurnal and multi-day to weekly fluctuations.

These results suggest that simulations based on a single condition (e.g. ventilation rate = 1) struggle to replicate the average $T_{in}$ within the same area, even when using process-based models such as SLUCM+BEM v2.0. It is therefore crucial to calculate the range and average from multiple experiments that vary the ventilation rate. Furthermore, observational data from a single room are likely to be heavily influenced by the specific conditions of that room, which makes it difficult to verify $T_{in}$ using similar models. When verifying the accuracy of process-based models such as SLUCM+BEM v2.0 that target $T_{in}$, it has been shown that either supplementary detailed data must be thoroughly recorded, such as measured ventilation rates, or data from multiple observation points within a certain spatial domain, as in the current dataset.

https://doi.org/10.5194/egusphere-2026-1307
Preprint. Discussion started: 1 April 2026


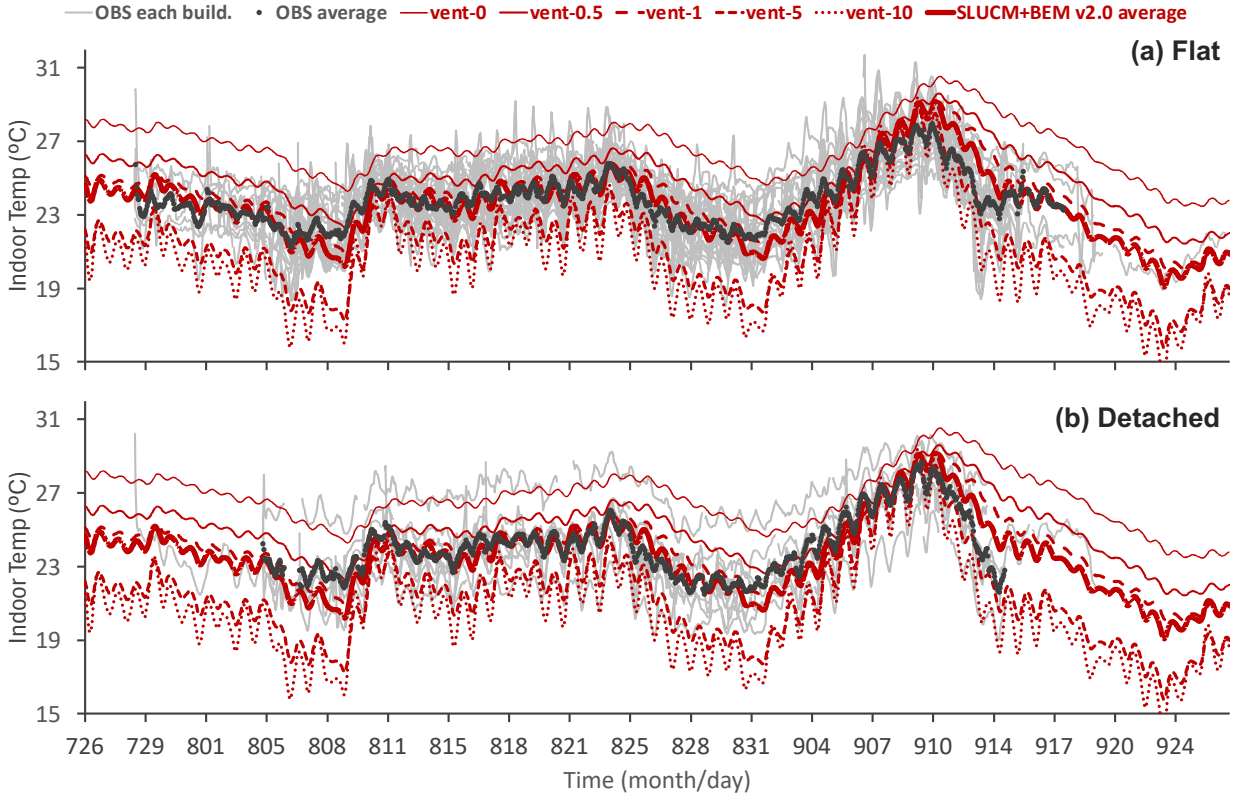


**Figure 4: Diurnal changes in indoor temperatures ($T_{in}$) in (a) flats and (b) detached buildings in Southwark, London, UK (Fig. 2) over the period 26 July to 30 September 2023. Light grey lines are observations in each room. The dark grey line is the average value. The red lines are the simulated values for each case; vent-0, 0.5, 1, 5 and 10, and the average value determined by SLUCM+BEM. MAE is mean absolute error; MBE is mean bias error; RMSE is root mean square error.**

### 3.2 Electricity consumption

Section 3.1 showed that SLUCM+BEM v2.0 can generally reproduce $T_{in}$ under natural ventilation conditions without AC. We next verified the $EC_{HAC}$ when HAC is used to bring $T_{in}$ closer to the setpoint. Because this would be impossible to achieve in London, where AC is not widespread, we conducted the study in the TMA, where SLUCM+BEM v1.0 and CM-BEM verifications had already been performed using observational data (Nakajima et al., 2022; Takane et al., 2023a). We used an online version of SLUCM+BEM v2.0 coupled with WRF to reproduce the horizontal distribution and temporal variation of $EC_{HAC}$ in the TMA during July–August 2018 and January–February 2017.

The summer results using v1.0 (Takane et al., 2024) are shown in Fig. 5, alongside the results from CM-BEM coupled with WRF (Kikegawa et al., 2014; Nakajima et al., 2023). As Takane et al. (2024) noted, v1.0 generally reproduces the horizontal

https://doi.org/10.5194/egusphere-2026-1307
Preprint. Discussion started: 1 April 2026


distribution of $EC_{HAC}$ in the TMA; however, it is evident that it overestimates $EC_{HAC}$, particularly in the central Tokyo office districts (BC) (see Figs. 5e and f versus a and b). The daily mean MBE in BC was 2.8 W floor-m$^{-2}$, and the MAE was 3.5 W floor-m$^{-2}$ (see Fig. 6). These values were higher than those for CM-BEM, which had an MBE of 2.1 W floor-m$^{-2}$ and an MAE of 2.5 W floor-m$^{-2}$. Conversely, v2.0 reduced the overestimation of BC in central Tokyo (Fig. 5c, d versus a, b). Specifically, the daily average MBE in BC was 0.5 W floor-m$^{-2}$, and the MAE was 1.7 W floor-m$^{-2}$, representing a significant improvement on v1.0's MBE of 2.8 W floor-m$^{-2}$ and MAE of 3.5 W floor-m$^{-2}$. The errors were now smaller than those of CM-BEM (see Fig. 6). Furthermore, the improvement in error was not limited to BC; Rm also improved (Fig. 6). Specifically, v1.0 had an MBE of 0.8 W floor-m$^{-2}$ and an MAE of 1.5 W floor-m$^{-2}$, whereas v2.0 had an MBE of -0.5 W floor-m$^{-2}$ and an MAE of 1.1 W floor-m$^{-2}$. No significant improvement was observed for Rd.

A reduction in the overestimation of $EC_{HAC}$ in BC was also observed during winter (see Figs 7 and 8). Specifically, v1.0 had an MBE of 1.1 W floor-m$^{-2}$ and an MAE of 2.1 W floor-m$^{-2}$, whereas v2.0 had an MBE of 0.0 W floor-m$^{-2}$ and an MAE of 1.5 W floor-m$^{-2}$.

When reproducing $EC_{HAC}$, it is important to consider not only horizontal distribution and temporal variation, but also the sensitivity of $EC_{HAC}$ to outdoor air temperature (used T2 as T) (temperature sensitivity: $\Delta EC_{HAC}/\Delta T$). Figure 9 shows the reproduction results. First, when examining the summer (high-temperature) plot for BC, the $\Delta EC_{HAC}/\Delta T$ (slope) in v1.0 was 0.848, which was > 0.2 higher than the observed value of 0.644. However, in v2.0, it was 0.556, reducing the difference from the observed value to within 0.1. Conversely, for the winter (low temperature) plot, v1.0 and v2.0 had values of -0.193 and -0.176, respectively, which were not improved upon compared to the observed value of -0.411. For Rm, the summer sensitivity in v2.0 was 0.138, i.e. worse than v1.0's 0.281 and the observed value of 0.249. For winter, v1.0 was -0.072, and v2.0 was -0.043, showing little change compared to the observed value of -0.138. For Rd, the $\Delta EC_{HAC}/\Delta T$ in summer was 0.082 for v2.0, which was unchanged from the value of 0.084 for v1.0; both of these values underestimated the observed value of 0.279. Similarly, in winter, v2.0 at -0.023 and v1.0 at -0.007 both underestimated the observed value of -0.165.

These results suggest that, although v2.0 improves the reproduction of $EC_{HAC}$ in BC, important limitations remain in residential areas, particularly in reproducing the temperature sensitivity of $EC_{HAC}$ ($\Delta EC_{HAC}/\Delta T$).

https://doi.org/10.5194/egusphere-2026-1307
Preprint. Discussion started: 1 April 2026


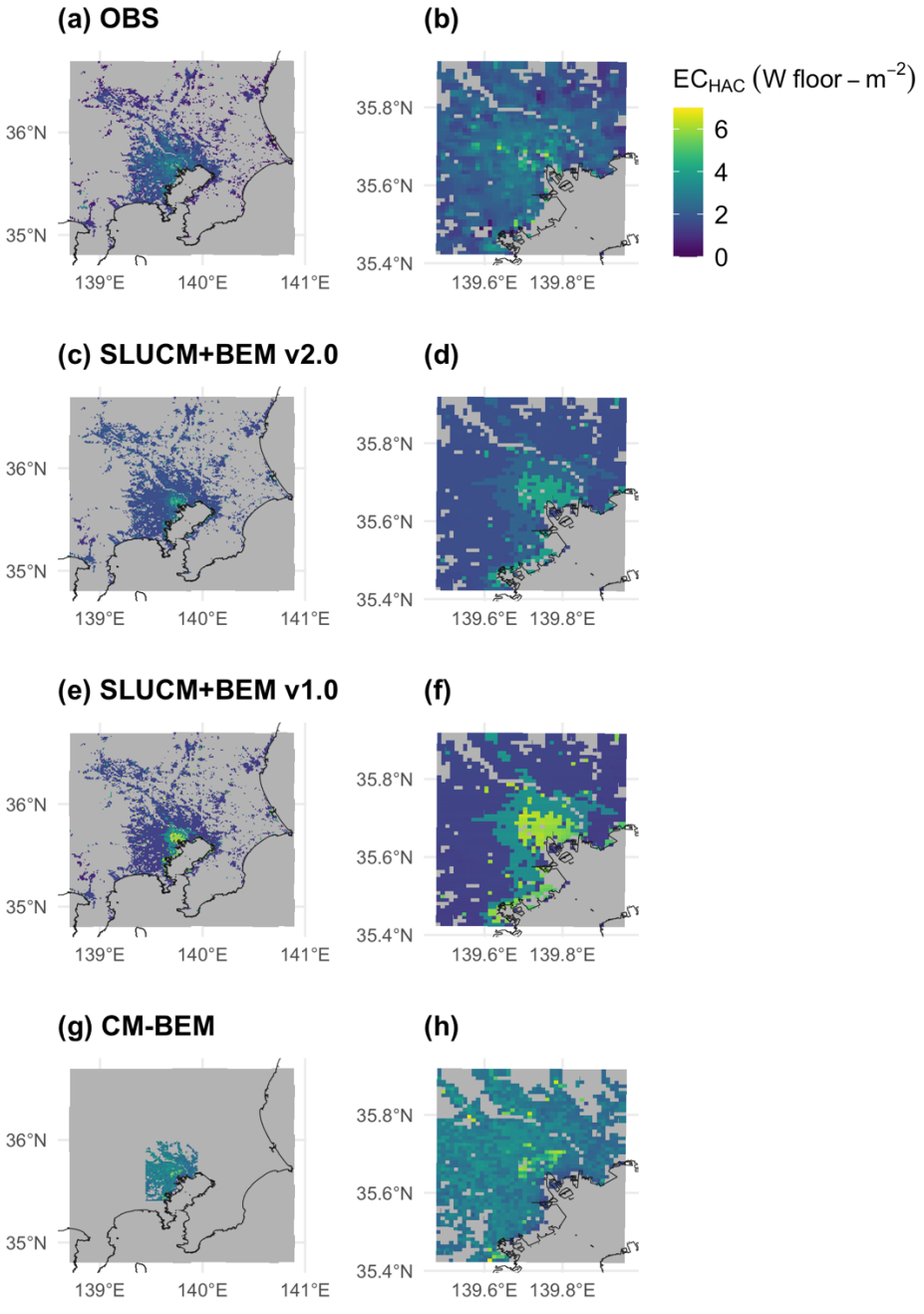


**Figure 5: Distributions of (a, b) observed and (c–h) simulated electricity consumption (EC) for heating and air conditioning (HAC) (i.e. $EC_{HAC}$) in the Tokyo metropolitan area (TMA) (a, c, e, g) and central Tokyo area (b, d, f, h) averaged over weekdays in summer. Simulation results from (c, d) SLUCM+BEM v2.0, (e. f) v1.0 and (g, h) CM-BEM.**

https://doi.org/10.5194/egusphere-2026-1307
Preprint. Discussion started: 1 April 2026


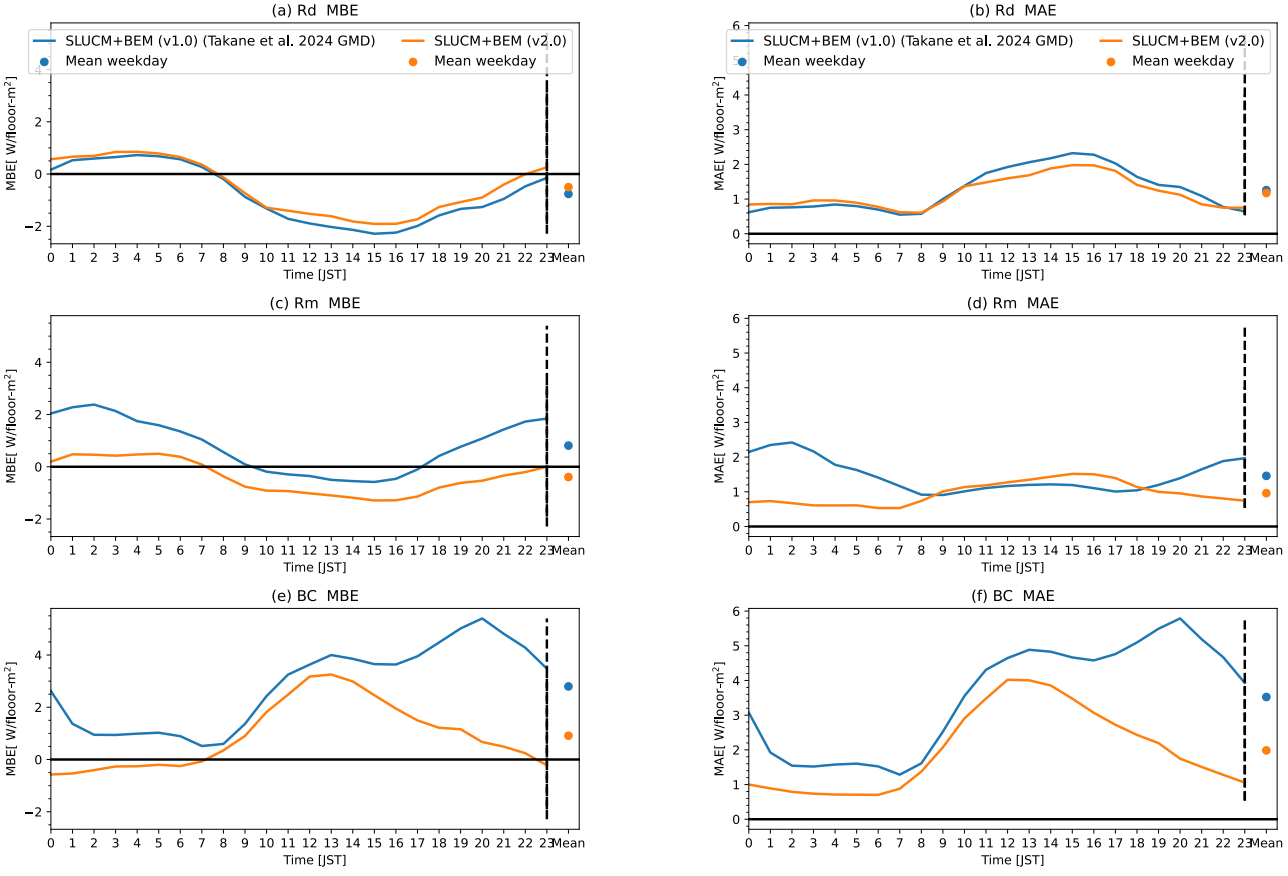


**Figure 6: Diurnal changes in the MBE (left) and MAE (right) of $EC_{HAC}$ for each type of urban building ((a, b) Rd, (c, d) Rm and (e, f) BC), and the average of all grids from SLUCM+BEM v1.0 (blue line and circle) and v2.0 (orange line and circle) averaged over the summer season's weekdays.**

https://doi.org/10.5194/egusphere-2026-1307
Preprint. Discussion started: 1 April 2026


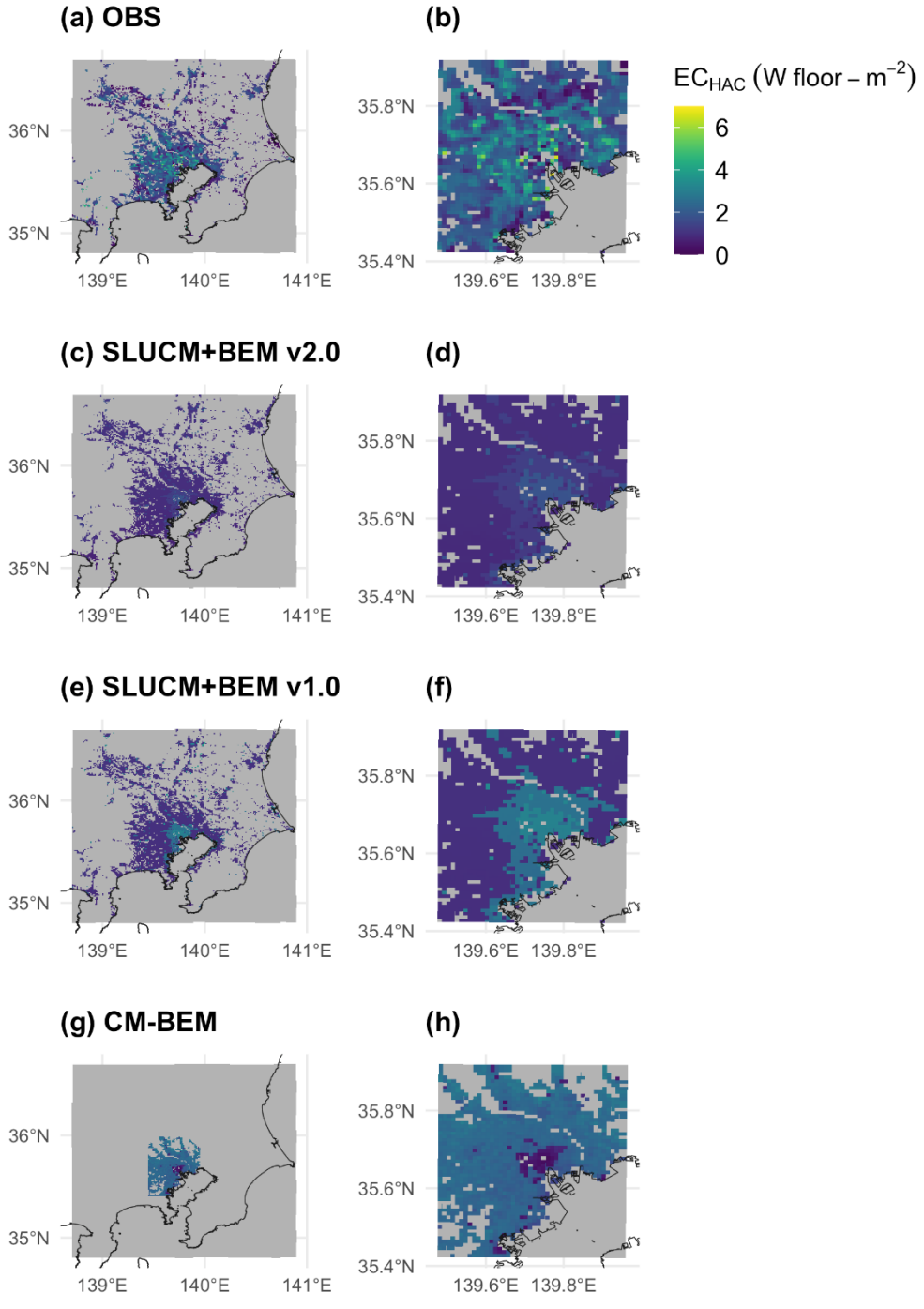


**Figure 7: As described for Fig. 4, but showing results for winter**

390

https://doi.org/10.5194/egusphere-2026-1307
Preprint. Discussion started: 1 April 2026


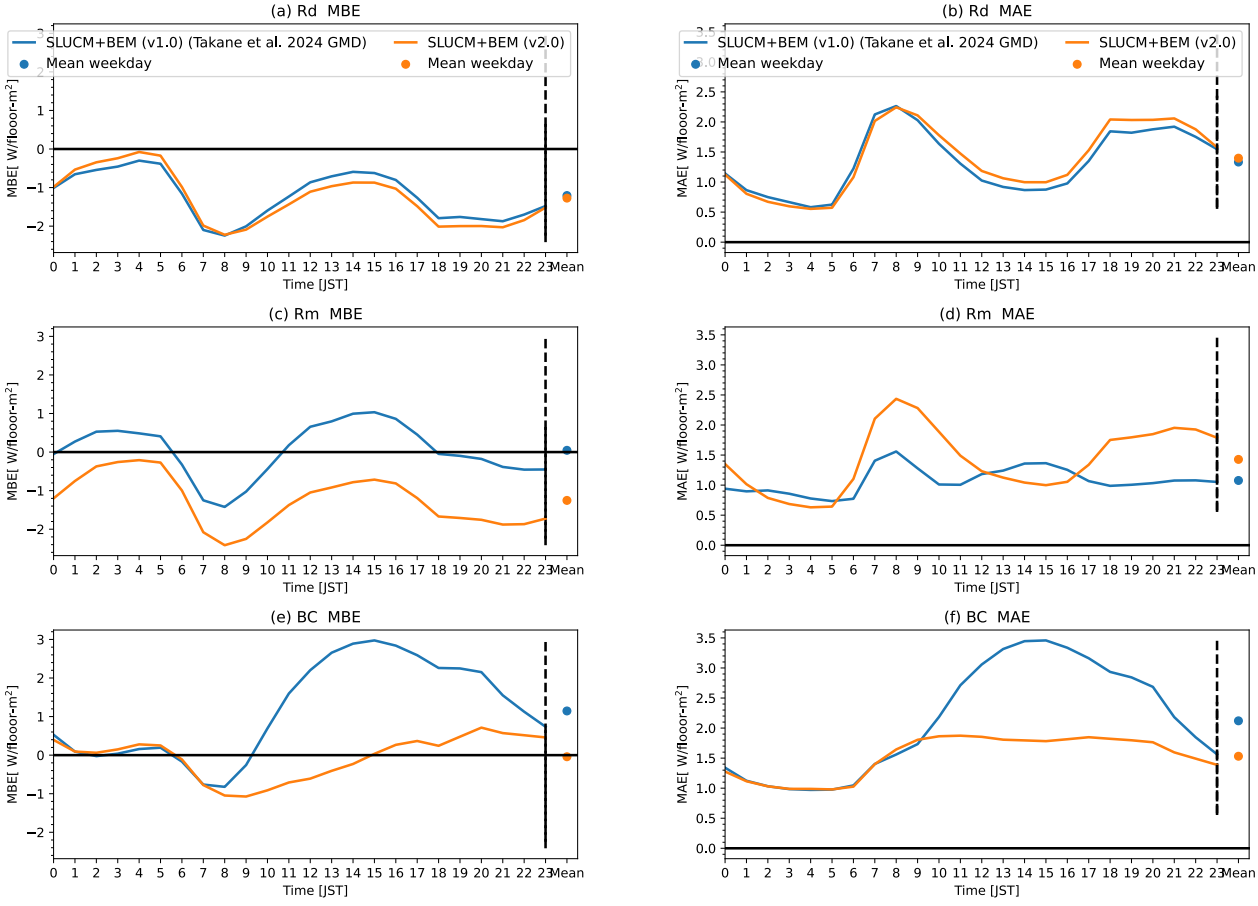


**Figure 8: As described for Fig. 5, but showing results for winter.**

https://doi.org/10.5194/egusphere-2026-1307
Preprint. Discussion started: 1 April 2026


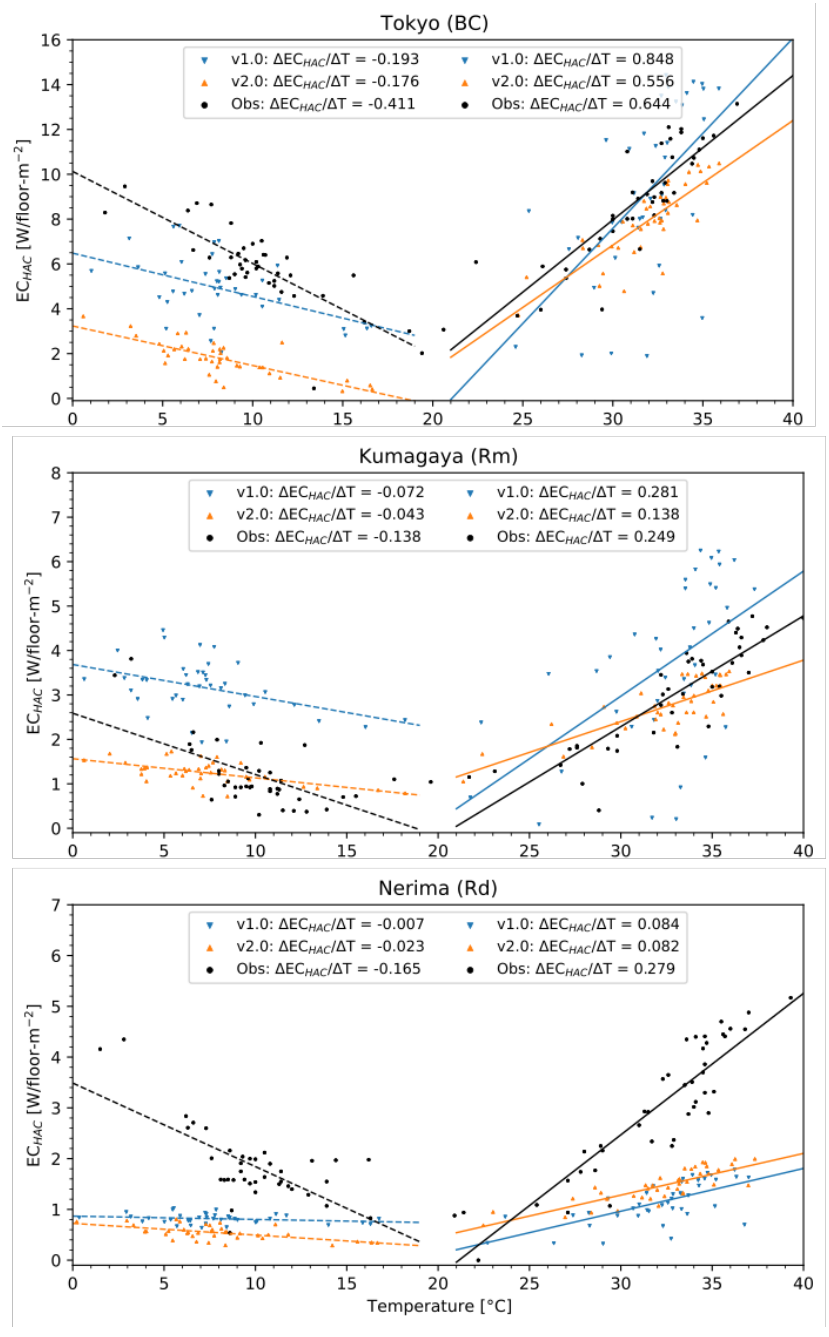


**Figure 9: Scatterplots of 2 m temperature and EC by HAC use ($EC_{HAC}$) in Tokyo (BC), Kumagaya (Rm), and Nerima (Rd) at 14:00 LT in summer and winter, simulated by SLUCM+BEM v1.0 (blue), v2.0 (orange), and the observation (black). Each plot shows daily results. Lines are single regression lines. Plots with temperatures > 20°C represent the results for summer; those with temperatures < 20°C represent the results for winter.**

395

https://doi.org/10.5194/egusphere-2026-1307
Preprint. Discussion started: 1 April 2026


### 3.3 Outdoor air temperature

Online simulations by SLUCM+BEM v2.0 coupled with WRF were used to reproduce not only $EC_{HAC}$, but also the outdoor air temperatures in major cities within the TMA during July–August 2018 and January–February 2017. These results, together with those reproduced by SLUCM+BEM v1.0 (Takane et al., 2024) and SLUCM, are presented in Table 4. As can be seen in the table, v2.0 reproduced outdoor temperatures with a similar level of accuracy to v1.0, regardless of season (summer or winter) or location (Tokyo, Kumagaya, or Nerima).

**Table 4: Verification of the 2 m temperature simulated by the SLUCM and SLUCM+BEM models (v1.0 and v2.0) for the cooling and heating seasons (summer and winter) in Tokyo (BC), Kumagaya (Rm), and Nerima (Rd).**

| Season | Place (Building-type) | Metric (ºC) | SLUCM[1] | SLUCM+BEM v1.0[2] | **SLUCM+BEM v2.0** |
|---|---|---|---|---|---|
| Summer | Tokyo (BC) | MBE | 0.56 | -0.24 | **-0.22** |
| | | MAE | 1.20 | 1.22 | **1.24** |
| | | RMSE | 1.77 | 1.62 | **1.65** |
| | Kumagaya (Rm) | MBE | -0.94 | -1.30 | **-1.26** |
| | | MAE | 1.74 | 1.92 | **1.92** |
| | | RMSE | 2.11 | 2.30 | **2.30** |
| | Nerima (Rd) | MBE | -0.56 | -0.99 | **-0.98** |
| | | MAE | 1.47 | 1.67 | **1.69** |
| | | RMSE | 1.84 | 1.99 | **2.02** |
| Winter | Tokyo (BC) | MBE | -0.59 | -2.24 | **-2.34** |
| | | MAE | 1.69 | 2.48 | **2.55** |
| | | RMSE | 2.06 | 2.85 | **2.92** |
| | Kumagaya (Rm) | MBE | -1.08 | -1.84 | **-1.78** |
| | | MAE | 1.88 | 2.24 | **2.20** |
| | | RMSE | 2.27 | 2.59 | **2.52** |
| | Nerima (Rd) | MBE | -1.65 | -2.38 | **-2.36** |
| | | MAE | 2.28 | 2.76 | **2.74** |
| | | RMSE | 2.69 | 3.20 | **3.17** |

BC, business and commercial building; Rm, residential area with multi-unit dwellings; Rd, residential area with detached dwellings; MBE, mean bias error; MAE, mean absolute error, RMSE, root mean square error.

[1] Kusaka et al. (2001)

[2] Takane et al. (2024)

https://doi.org/10.5194/egusphere-2026-1307
Preprint. Discussion started: 1 April 2026


## 4 Discussion

### 4.1 Improvement of the indoor heat load ($H_{in}$)

Section 3.2 showed that v2.0 enhanced the accuracy of $EC_{\mathrm{HAC}}$ 's reproduction of horizontal distribution, temporal variation, and temperature sensitivity, particularly in BC. Here, we examine the factors contributing to this enhancement. The most notable difference between v1.0 and 2.0 lies in the method used to calculate the indoor heat load $H_{in}$ (Fig. 1, Eqs. 2 and 21). In v1.0, apart from the base load (i.e. the internal heat load from occupants and equipment), only the heat transfer through the wall and roof, calculated using the interior wall surface and ceiling temperatures as boundary conditions, was considered. In v2.0, this was expanded to include convective and radiative heat transport from interior walls and the ceiling, accounting for differences in $T_{in}$, as well as heat load due to ventilation.

The components constituting $H_{in}$ are plotted in Fig. 10. First, examining the time variation of BC in v1.0 during summer revealed that $H_{in}$ remained constant regardless of time. This was due to the balancing of $qE$ and $qHS$, which exhibited diurnal variation (small at night and in the morning, large during the day), and HTRANS, which showed the opposite trend. Conversely, examining the BC calculation results from v2.0 showed that $H_{in}$ exhibited a clear diurnal variation (large during the day and small at night and in the morning). This diurnal variation was consistent with the results of CM-BEM (Nakajima et al., 2023), which uses a more detailed BEM (Kikegawa et al., 2003) (see Fig 10). $Q_{VENT}$ significantly influences this variation. Section 3.2 showed that the v1.0 boundary conditions resulted in the $EC_{\mathrm{HAC}}$'s MBE exceeding 4 W floor-m$^{-2}$ after 13:00, with this value increasing further after 17:00 to reach 5.4 W floor-m$^{-2}$ by 20:00 (Fig. 6e). Conversely, in v2.0, the MBE remained below 2 W floor-m$^{-2}$ after 16:00, representing a significant improvement in accuracy. The primary cause of the significant error in v1.0 during the evening and night was assumed to be $H_{in}$ remaining elevated throughout the night. For Rm and Rd in v1.0, $H_{in}$ tended to be nearly constant throughout the day, or even slightly smaller during the daytime (see Fig. 10), whereas in v2.0 it now exhibited a clear diurnal variation, with significantly higher values during the day and lower values from the night into the morning, similar to the BC.

Although these results are from summer calculations, analogous trends occurred during winter (Fig. 11). Specifically, v1.0 exhibited a constant $H_{in}$ throughout the winter day, regardless of sign, whereas v2.0 again demonstrated a clear diurnal variation.

As described above, the introduction of the ventilation process has made the diurnal variation in $H_{in}$ as pronounced as in the existing detailed model. This enhancement in the representation of $H_{in}$ is a key reason for the improved accuracy in reproducing the horizontal distribution and temporal variation of $EC_{HAC}$, particularly in the BC.

https://doi.org/10.5194/egusphere-2026-1307
Preprint. Discussion started: 1 April 2026


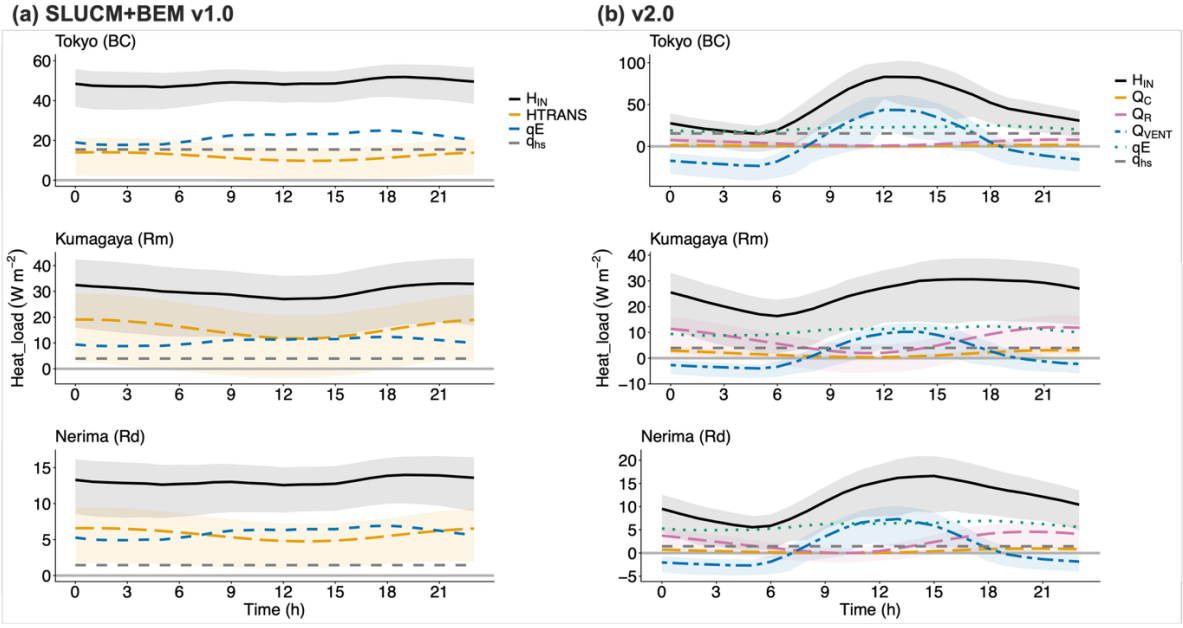


**Figure 10: Diurnal changes in each component of indoor heat load $H_{in}$ (Eqs. 2 and 21) in Tokyo (BC), Kumagaya (Rm), and Nerima (Rd; Fig. 3b) simulated by SLUCM+BEM (a) v1.0 and (b) v2.0 averaged seasonally over summer. Lines and ribbons indicate the simulated mean and 5$^{th}$ and 95$^{th}$ percentiles.**

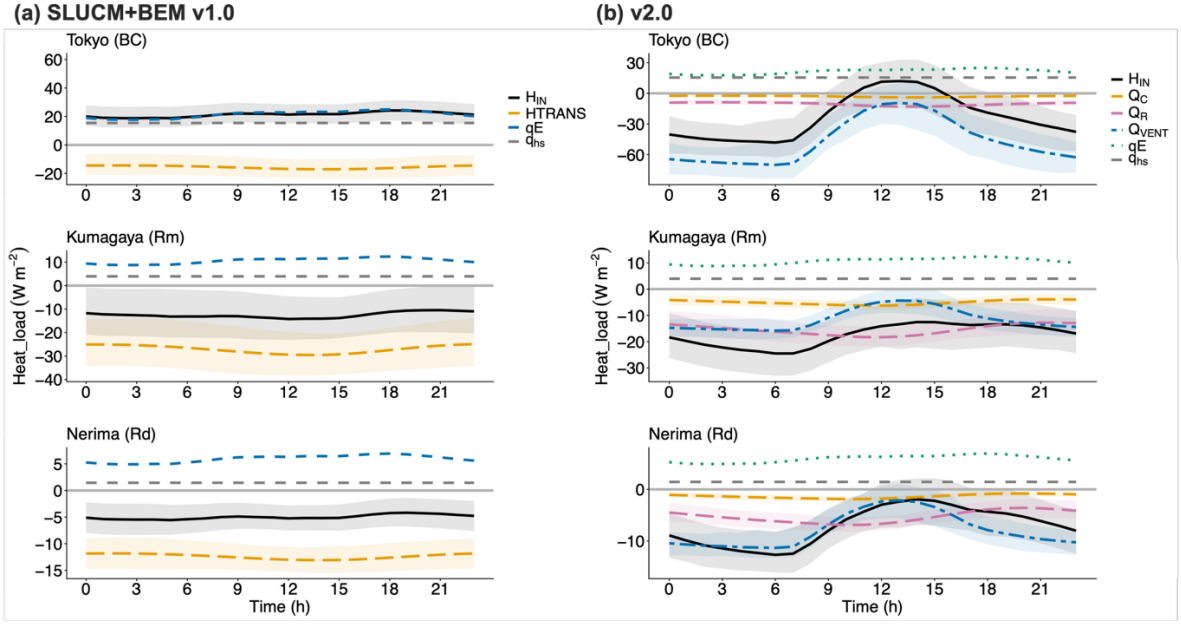


**Figure 11: As described for Fig. 10, but showing results for winter.**

https://doi.org/10.5194/egusphere-2026-1307
Preprint. Discussion started: 1 April 2026


### 4.2 Evaluation of heating and air conditioning use as an adaptation strategy on $Q_{FB\_S}$, T2, and $T_{in}$

In v2.0, it became possible to calculate $T_{in}$ under natural ventilation conditions, and it was confirmed that this modelled $T_{in}$ could replicate, to some extent, the indoor temperatures observed in the Southwark area of London (section 3.1). This means that simulations can now be performed for two distinct cases: one with AC and one without. Consequently, it is now possible to evaluate the impact of $Q_{FB}$ from HAC use on EC, $T_{in}$, and outdoor temperature as an adaptation measure. Furthermore, it is now possible to assess and predict the rise in $T_{in}$ without AC in cities exposed to high temperatures, such as those in Japan.

Here, we present an example evaluation using this model. Specifically, we evaluated a "what if" scenario for the TMA: what would the outdoor and $T_{in}$ be if HAC was not used, compared to a control case where it is used? This scenario is representative of a plausible situation, such as a power outage caused by a disaster such as a typhoon (e.g. Yamasaki et al., 2024) or earthquake. Figure 12 shows the summer results. Without AC, the $Q_{FB\_S}$ decreased by an average of approximately 40 W m$^{-2}$, particularly during the daytime in the BC case. On some days, a decrease of 50 W m$^{-2}$ was observed (see Fig. 11a). Decreases were also observed throughout the day for Rm and Rd. This reduction in $Q_{FB\_S}$ led to a decrease in the outdoor air temperature. Specifically, for BC, a decrease of > -0.2°C was observed from daytime into the night. On some days, the decrease exceeded -1°C (Fig. 12b). Conversely, these results indicate that AC increases $Q_{FB\_S}$, raising the outdoor air temperature by an average of 0.2°C or more and, on some days, by over 1°C. The magnitude of this impact (0.2–1°C) is consistent with values reported in previous studies investigating the effect of exhaust heat on air temperature (e.g. Ohashi et al., 2007; Salamanca et al., 2014; Takane et al., 2019, 2020, 2022). Not using AC reduced $Q_{FB\_S}$, thereby lowering the outdoor temperature. However, $T_{in}$ increased by over 3°C during the day and by approximately 1°C in the early morning, regardless of building use (see Fig. 12c). In Japan, over half of all heatstroke fatalities occur indoors, with a significant proportion happening in the absence of AC. SLUCM+BEM v2.0 can simulate $T_{in}$ in such scenarios, enabling evaluation, prediction, and research into countermeasures to address this societal issue – a significant advantage of v2.0.

Winter results essentially exhibited the opposite pattern to summer. Specifically, not using HAC caused a slight increase in $Q_{FB\_S}$ due to the reduced heat absorption (negative heat discharge) from the heat pump HAC. $T_{in}$ decreased by over 4°C in BC and by almost 7°C in Rm and Rd. However, the impact of this slight increase in $Q_{FB\_S}$ on the outdoor temperature was not clearly evident (figure omitted).

https://doi.org/10.5194/egusphere-2026-1307
Preprint. Discussion started: 1 April 2026


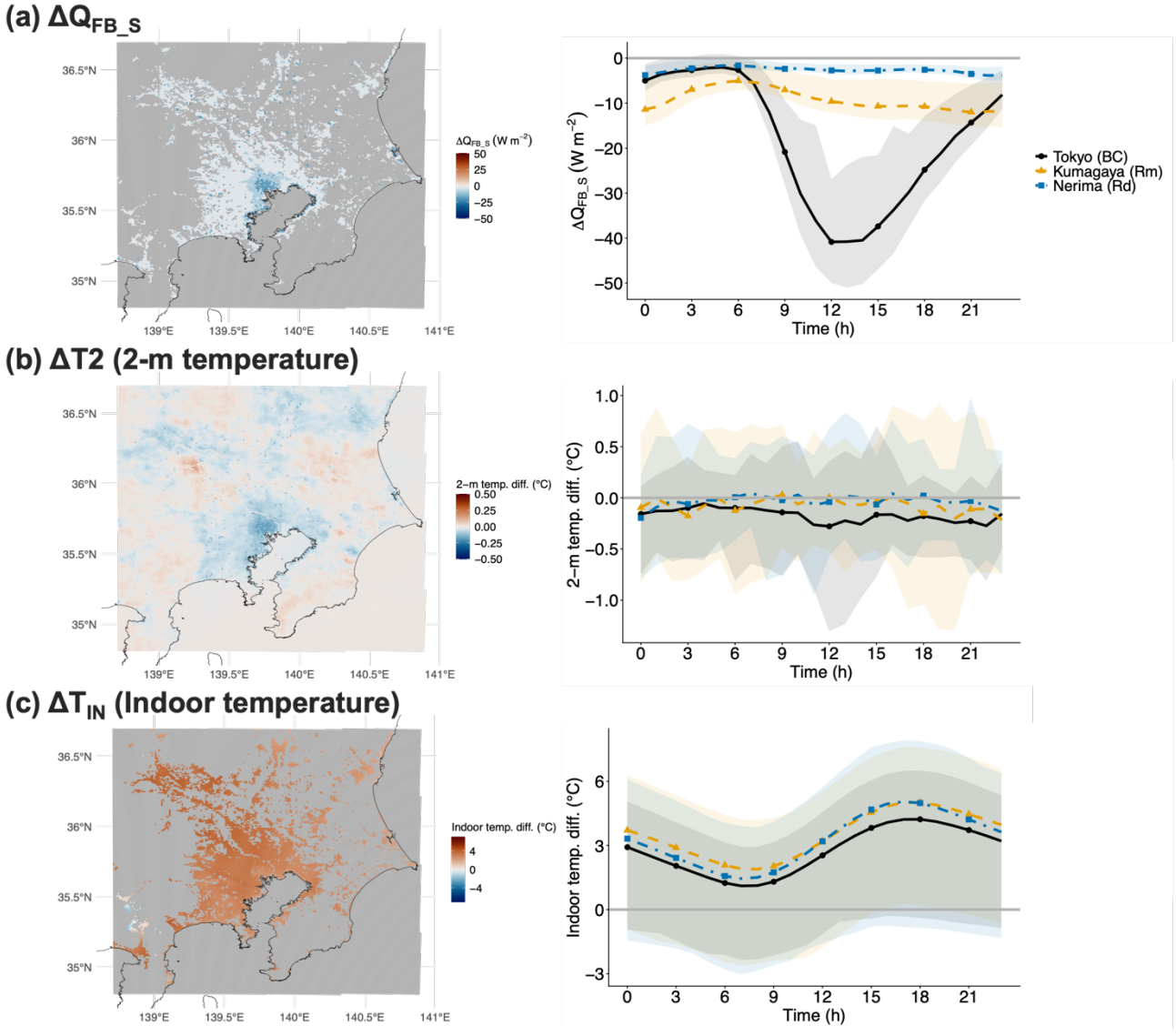


**Figure 12: Average SLUCM+BEM-simulated difference of (a) $Q_{FB\_S}$, (b) 2-m temperature, and (c) indoor temperature ($T_{in}$) between no-HAC and CTRL in distributions over the Tokyo metropolitan area (TMA) averaged at 00:00–23:00 LT in summer as obtained from SLUCM+BEM (left). Diurnal changes in the difference of $\Delta Q_{FB\_S}$, 2-m temperature and $T_{in}$ in values for Tokyo (BC), Kumagaya (Rm), and Nerima (Rd) (right). The lines and ribbons indicate the simulated mean and the 5$^{th}$ and 95$^{th}$ percentiles, respectively.**

### 4.3 Practical implementation in WRF and compatible schemes and input data for SLUCM+BEM v2.0

All simulations presented in this paper were conducted with WRF v4.3.2, Noah-LSM, and Japan's National Land Numerical Information dataset (three urban categories), using the SLUCM+BEM v2.0 implementation described in Section 2. To make

https://doi.org/10.5194/egusphere-2026-1307
Preprint. Discussion started: 1 April 2026


the implementation more practical for readers, Fig. 13 provides a schematic overview of the modified WRF modules and compatible options, while Table 5 summarizes the tested configurations, required user settings, and modified source files.

To avoid ambiguity, we distinguish here between (i) the configuration used for the scientific evaluation presented in this paper and (ii) additional configurations tested for implementation compatibility. In this study, the scientific evaluation was performed with WRF v4.3.2, Noah-LSM, and Japan's National Land Numerical Information dataset. In addition, implementation compatibility of SLUCM+BEM v2.0 was tested for WRF v4.5.1, v4.6.1, and v4.7.1. Here, "implementation compatibility" means that the required modified source files could be compiled successfully and that WRF ran stably with the corresponding settings.

SLUCM+BEM v2.0 was tested with both Noah-LSM and Noah-MP. It also remains compatible with the hydrological processes implemented in SLUCM (Yang et al., 2015; 2016), allowing the model to evaluate rooftop greening and its effects on outdoor air temperature, indoor heat load, and anthropogenic heat emissions. The specific source files modified for each supported option are listed in Table 5.

At the WPS/input-data level, SLUCM+BEM v2.0 was used in this study with Japan's National Land Numerical Information dataset and was also confirmed to be compatible with the default MODIS land-use dataset, LCZ (Demuzere et al., 2022), and distributed urban parameters for SLUCM (Vázquez et al., 2021; Khanh et al., 2023). Thus, once the corresponding modified source files are applied, users can switch among supported land-surface models and urban input datasets by changing standard namelist.input and URBPARM.TBL / URBPARM_LCZ.TBL settings, without additional structural modification of the SLUCM+BEM v2.0 code. Practical reproduction guidance is provided in Supplementary Text S1 and Supplementary Table S1.

https://doi.org/10.5194/egusphere-2026-1307
Preprint. Discussion started: 1 April 2026


**Table 5: Practical implementation summary of SLUCM+BEM v2.0 in WRF, including supported options, required user settings, and modified source files. "Used in this study" refers to the configuration employed for the scientific evaluation presented in this paper. "Implementation compatibility tested" denotes successful compilation and stable execution with the specified option.**

| Category | Option / configuration | Where the user selects it | Required setting / selection | Modified files / key implementation files | Status / note |
|---|---|---|---|---|---|
| WRF version | v4.3.2 | – | – | Version-specific modified files | **Used in this study** |
| WRF version | v4.5.1 | – | – | Version-specific modified files | Implementation compatibility tested |
| WRF version | v4.6.1 | – | – | Version-specific modified files | Implementation compatibility tested |
| WRF version | v4.7.1 | – | – | Version-specific modified files | Implementation compatibility tested |
| Land surface model | Noah-LSM | namelist.input (&physics) | sf_surface_physics = 2 | module_sf_noahdrv.F; module_surface_driver.F | **Used in this study**; implementation compatibility tested |
| Land surface model | Noah-MP | namelist.input (&physics) | sf_surface_physics = 4 | module_sf_noahmpdrv.F; module_surface_driver.F | Implementation compatibility tested |
| Urban physics | SLUCM+BEM v2.0 | namelist.input (&physics) / URBPARM.TBL / URBPARM_LCZ.TBL | sf_urban_physics = 1 Set SBEMOPTION, AH_TRAFFIC, AHDIUPRF, TARGTEMP, HSEQUIP_SCALE_FACTOR, HSEQUIP, AB_BUILD_RATIO, AC_FLOOR_RATIO, AC_USAGE_RATIO_CL, AC_USAGE_RATIO_HT, COPOPTION. COP, and VENT_RATE as required | module_sf_urban.F; URBPARM.TBL / URBPARM_LCZ.TBL | **Used in this study**; implementation compatibility tested |
| Urban physics | Urban hydrological processes | namelist.input (&physics) / URBPARM.TBL / URBPARM_LCZ.TBL | sf_urban_physics = 1 Set ALHOPTION, ALHSEASON, ALHDIUPRF, IMP_SCHEME, IRI_SCHEME, GROPTION, and FGR as required | module_sf_urban.F; URBPARM.TBL / URBPARM_LCZ.TBL | Implementation compatibility tested |
| Urban input data | Japan's National Land Numerical Information dataset (3 urban categories) | WPS / geogrid input | Select Japan dataset | No additional WPS source modification required | **Used in this study** |
| Urban input data | MODIS | WPS / geogrid input | Select default MODIS dataset | No additional WPS source modification required | Implementation compatibility tested |
| Urban input data | LCZ | WPS / geogrid input and URBPARM_LCZ.TBL | Select LCZ dataset and use URBPARM_LCZ.TBL | No additional WPS source modification required | Implementation compatibility tested |
| Urban input data | Distributed urban parameters for SLUCM | WPS / geogrid input | Select distributed urban parameters | No additional WPS source modification required | Implementation compatibility tested |

Note. "Implementation compatibility tested" indicates successful compilation and stable execution with the specified configuration. All scientific analyses presented in this paper were conducted with WRF v4.3.2, Noah-LSM, and Japan's National Land Numerical Information dataset.

https://doi.org/10.5194/egusphere-2026-1307
Preprint. Discussion started: 1 April 2026


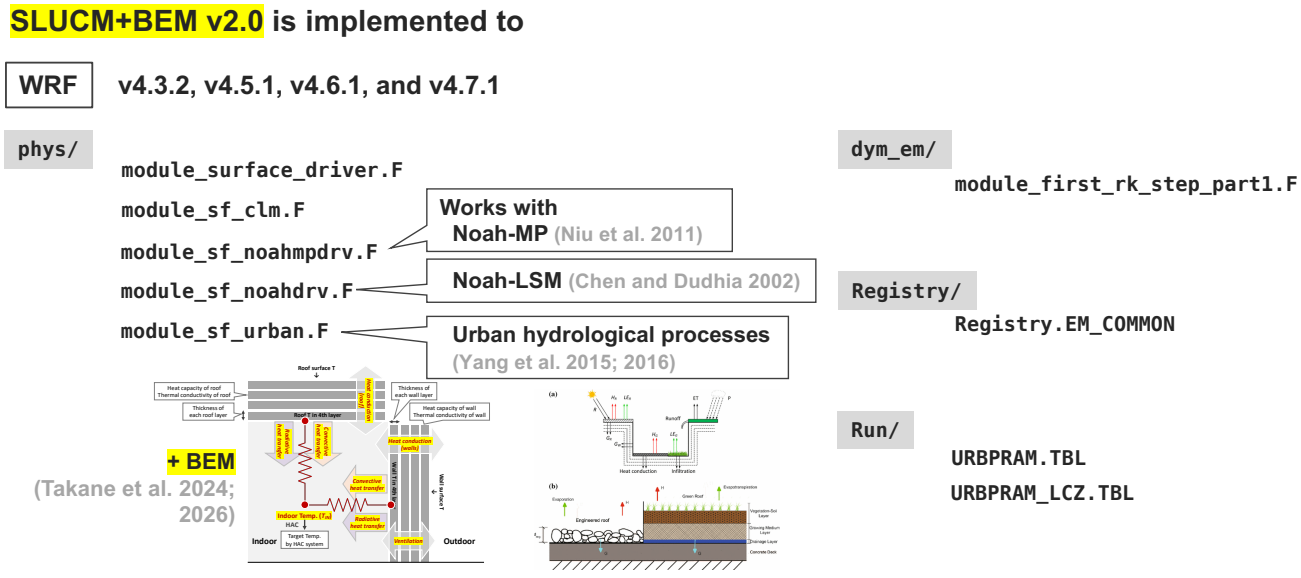


**Figure 13: Modified codes in WRF (v4.3.2, 4.5.1, 4.6.1, and 4.7.1), and schemes compatible with SLUCM+BEM v2.0.**

### 4.4 Limitations and future studies

Finally, we summarise the current strengths and weaknesses of SLUCM+BEM v2.0, as well as the future challenges. The strengths are as follows:

- When used online with WRF, SLUCM+BEM v2.0 achieves computational speeds comparable to those of the original SLUCM. The existing BEP+BEM and CM-BEM models were found to require 2.3 and 1.7 times the computational time, respectively, compared to SLUCM+BEM v2.0 (see Table 1). These benchmarks were obtained under the computational environment of CPU: AMD EPYC 7763 × 2; cores: 128 (64 × 2); memory: 1 TB; using 36-core parallel processing, as in the comparative experiments by Kikegawa et al. (2025). Although these ratios may vary depending on hardware, SLUCM+BEM v2.0's faster performance was considered robust.
- The $EC_{HAC}$ reproduction accuracy achieved by SLUCM+BEM v2.0 was a significant improvement on that of v1.0, and was comparable to the highly detailed existing model, CM-BEM (see section 3.2).
- Regarding $T_{in}$, this study is likely the first to verify the accuracy of this type of model, or at least the first to verify it in a very limited case.
- SLUCM+BEM v2.0 is also simple in terms of coding. The main coding additions were primarily made as subroutines within "module_sf_urban.F", totalling approximately 900 lines (about 20% of the original total).
- Both an online version for use with WRF and an offline version portable to other models are available.

https://doi.org/10.5194/egusphere-2026-1307
Preprint. Discussion started: 1 April 2026


The limitations and challenges of this model are summarised below:

- Section 3.2 demonstrated that SLUCM+BEM v2.0 primarily underestimates the temperature sensitivity of $EC_{HAC}$ in residential areas (Rd, Rm). In particular, in Rm, the summer sensitivity in v2.0 was even lower than that in v1.0, and in both Rm and Rd the sensitivities in summer and winter remained substantially smaller than observed. This indicates that introducing prognostic $T_{in}$ and ventilation alone is not sufficient to reproduce the observed residential response. One plausible reason is that the model does not account for solar heat gain, especially transmitted shortwave radiation through windows, which can contribute substantially to the indoor heat load ($H_{in}$) in residential buildings during hot and sunny periods. At the same time, because a substantial mismatch also remains in winter, omitted solar heat gain alone may not fully explain the discrepancy. Accordingly, the current version is more suitable for broad-area urban climate and EC assessments, and for office/commercial districts where clear improvement was obtained, than for detailed quantitative prediction of the temperature sensitivity of residential $EC_{HAC}$. A key challenge for future development is therefore to incorporate solar heat gain transmitted through windows in as simple a manner as possible.
- As SLUCM is a single-layer model, it cannot calculate the impact of countermeasures at different heights within the urban canopy layer. It also cannot calculate $T_{in}$, outdoor temperature, or wind profiles, unlike BEP+BEM or CM-BEM.
- Although SLUCM incorporates roof greening and irrigation models (Yang et al., 2015, 2016), it lacks certain application-side options such as solar panels, which are included in BEP+BEM, CM-BEM, and other models (e.g. Zonato et al., 2021; Sun et al., 2026; Chen et al., 2021).
- Indoor latent heat load (e.g. Kikegawa et al. 2003; Meili et al. 2025) is not considered.
- Anthropogenic heat is not directly reflected in the estimated urban canopy temperature (Li et al. 2024c).
- Verification of $T_{in}$ remains necessary, although this is not unique to SLUCM+BEM v2.0, but rather a challenge for all similar models.
- Application across a diverse range of global cities remains necessary, as does coupling with global climate models (e.g. Oleson and Feddema 2020; Zhao et al. 2014; Li et al. 2024).
- Expansion of use for the evaluation of climate change adaptation measures and future projections is required.

## 5 Summary

This model operates coherently with land surface models integrated into WRF and hydrological processes incorporated into SLUCM. It also functions when combined with SLUCM-specific distributed parameters and land use input data, such as the LCZ. Key features include a computational load that is comparable to that of SLUCM and less than half that of similar models. However, several challenges remain. Most importantly, the current version is more suitable for broad-area assessments and for office/commercial districts than for detailed quantitative prediction of the temperature sensitivity of residential $EC_{HAC}$. In

https://doi.org/10.5194/egusphere-2026-1307
Preprint. Discussion started: 1 April 2026


particular, solar heat gain and indoor humidity loads are not yet considered explicitly, and the duration and locations available for verifying $T_{in}$ accuracy remain limited.

We have developed and released SLUCM+BEM v2.0, a new model that is capable of accurately simulating urban climates and EC over broad areas, and at speeds faster than conventional urban canopy building energy models.

The original version (v1.0) simplified the model by setting the boundary conditions for wall and roof temperatures to the HAC setpoint. This prevented the calculation of indoor temperatures ($T_{in}$) under natural ventilation conditions (i.e. without HAC), limiting its applicability to wider regions and scenarios. This simplification was also considered a key reason for the overestimation of EC in office districts of Tokyo (MAE = 3.5 W floor$^{-2}$ in summer, 2.1 W floor$^{-2}$ in winter).

To address these issues, this study introduced a new version (v2.0) of the model in which $T_{in}$ varies according to HAC usage, outdoor temperatures, and ventilation conditions.

This enables v2.0 to calculate $T_{in}$ under natural ventilation conditions. $T_{in}$ under natural ventilation conditions was calculated for a residential area in London and compared with observed values. The results showed that v2.0 generally reproduced the range of uncertainty, diurnal variations, and temporal changes in $T_{in}$ in the area over periods ranging from days to weeks, with MAE = 0.63–0.65ºC.

Furthermore, the accuracy of reproducing the EC associated with HAC usage in the TMA was verified. The results showed a significant improvement in the overestimation of EC in office districts by v1.0 (MAE = 1.7 W floor$^{-2}$ in summer, 1.5 W floor$^{-2}$ in winter), with values lower than those of the similar but more detailed CM-BEM (MAE = 2.5 W floor$^{-2}$ in summer). This significant improvement was due to the elimination of the previously simplified HAC setpoint temperature and the introduction of $T_{in}$ modelling, as well as the introduction of ventilation processes when calculating the thermal load within buildings. However, Section 3.2 also showed an important remaining limitation in residential areas. In the residential categories (Rm and Rd), the simulated temperature sensitivity of $EC_{HAC}$ with respect to outdoor air temperature remained substantially smaller than observed in both summer and winter, and in Rm the summer sensitivity in v2.0 was even lower than in v1.0. This indicates that the introduction of $T_{in}$ modelling and ventilation processes alone is not sufficient to reproduce the observed residential response. A plausible reason is the omission of solar heat gain, especially transmitted shortwave radiation through windows, although this factor alone may not fully explain the winter discrepancy.

Upgrading from SLUCM+BEM v1.0 to v2.0 enabled climate change adaptation measures to be evaluated, such as the introduction of HAC, in both indoor and outdoor environments. Consequently, the interaction between indoor and outdoor climates and human activities became calculable, including the increase in outdoor temperature due to anthropogenic heat ($Q_F$) emissions. Specifically, quantifying the difference between air-conditioned and non-air-conditioned conditions in the TMA

https://doi.org/10.5194/egusphere-2026-1307
Preprint. Discussion started: 1 April 2026


revealed that, without AC, $Q_F$ emissions decreased by an average of 40 W m$^{-2}$ during the day. This led to an average outdoor temperature reduction of 0.2°C daily, with reductions exceeding 1°C on some days. Conversely, $T_{in}$ increased by over 3°C during the day and approximately 1°C in the early morning, regardless of building type.

This model operates coherently with land surface models integrated into WRF and hydrological processes incorporated into SLUCM. It also functions when combined with SLUCM-specific distributed parameters and land use input data, such as the LCZ. Key features include a computational load that is comparable to that of SLUCM and less than half that of similar models. However, several challenges remain. Most importantly, the current version is more suitable for broad-area assessments and for office/commercial districts than for detailed quantitative prediction of the temperature sensitivity of residential $EC_{HAC}$. In particular, solar heat gain and indoor humidity loads are not yet considered explicitly, and the duration and locations available for verifying $T_{in}$ accuracy remain limited.

The SLUCM+BEM v2.0 code is available as an online version coupled with WRF, as well as a standalone version. Both are freely downloadable, providing new options for WRF and standalone SLUCM users.

## Code and data availability

The code and the data sources used in this work are publicly available as follows. The WRF model may be downloaded from https://github.com/wrf-model/WRF (last access: 9 March 2026). The Unified Noah LSM may be downloaded from https://ral.ucar.edu/model/unified-noah-lsm (last access: 9 March 2026). The exact archived version of the WRF-SLUCM+BEM source code used in this study (WRF v4.3.2 coupled with SLUCM+BEM v2.0) is available on Zenodo at https://doi.org/10.5281/zenodo.18918749 (Takane and Kikegawa, 2026). The input data used for the evaluation over the Tokyo Metropolitan Area are archived on Zenodo at https://doi.org/10.5281/zenodo.10685693 (Takane et al., 2024b). The observation data of indoor temperature used for the evaluation in London are available from https://data.ubdc.ac.uk/datasets/cc9cb186-e090-46e9-9d5b-b57a332a08a4 (last access: 28 March 2026). The Zenodo software archive is distributed under the Creative Commons Attribution 4.0 International (CC BY 4.0) licence. Details of the modified WRF modules, tested configurations, and practical implementation settings are provided in Section 4.3, Table 5, and Supplementary Table S1.

## Author contributions

YT and YK designed the study, and YT led the development of WRF–SLUCM+BEM v2.0, with significant contributions from YK. YT performed the evaluation. ZL and SG provided the indoor temperature measurement data. YT, YK, and HK drafted the manuscript, and all authors reviewed and edited the manuscript.

https://doi.org/10.5194/egusphere-2026-1307
Preprint. Discussion started: 1 April 2026


## Competing interests

The authors declare that they have no conflict of interest.

## Acknowledgements

This study was supported by the Environmental Research and Technology Development Fund (grant no. JPMEERF20231007 and JPMEERF25S12433) of the Environmental Restoration and Conservation Agency (ERCA) of Japan. We were also supported by a Japan Society for the Promotion of Science (JSPS) KAKENHI grant (no. JP23H01544, JP25K00040, JP23H00540 and JP24H00336) and the Japan Science and Technology Agency (JST) FOREST Program (Grant Number JPMJFR241G, Japan). The calculations were performed using the supercomputer system (HPE Apollo 2000) of the National Institute for Environmental Studies. We thank Dr Ko Nakajima of the National Institute of Advanced Industrial Science and Technology for his technical support using the electricity consumption data. We also thank Dr Cenlin He of the NSF National Center for Atmospheric Research (NCAR) for his advice on the implementation of WRF.

## Financial support

This study was supported by the Environmental Research and Technology Development Fund (grant no. JPMEERF20231007 and JPMEERF25S12433) of the Environmental Restoration and Conservation Agency (ERCA) of Japan, Japan Society for the Promotion of Science (JSPS) KAKENHI grant (no. JP23H01544, JP25K00040, JP23H00540 and JP24H00336), and by the Japan Science and Technology Agency (JST) FOREST Program (Grant Number JPMJFR241G, Japan).

## References

Brousse, O., Simpson, C., Kenway, O., Martilli, A., Krayenhoff, E. S., Zonato, A., and Heaviside, C.: Spatially explicit correction of simulated urban air temperatures using croudsouced data. Journal of Applied Meteolorogy and Climatology, 62, 1539–1572. doi: 10.1175/JAMC-D-22-0142.1, 2023.

Bueno, B., Pigeon, G., Norford, L. K., Zibouche, K., and Marchadier, C.: Development and evaluation of a building energy model integrated in the TEB scheme. Geoscientific Model Development, 5(2), 433–448. doi:10.5194/gmd-5-433-2012, 2012.

Capel-Timms, I., Smith, S. T., Sun, T., and Grimmond, S.: Dynamic Anthropogenic activitieS impacting Heat emissions (DASH v1.0): development and evaluation, Geosci. Model Dev., 13, 4891–4924, doi:10.5194/gmd-13-4891-2020, 2020.

Chao, Y., Li, Z., Farrara, J. D., and Hung, P.: Blending sea surface temperatures from multiple satellites and in situ observations for coastal oceans. Journal of Atmospheric and Oceanic Technology, 26(7), 1415–1426. doi:10.1175/2009JTECHO592.1, 2009.

https://doi.org/10.5194/egusphere-2026-1307
Preprint. Discussion started: 1 April 2026


Chen, F., and Dudhia, J.: Coupling and advanced land surface-hydrology model with the Penn State-NCAR MM5 modeling system. Part I: Model implementation and sensitivity. Monthly Weather Review, 129(4), 569–585. doi:10.1175/1520-0493(2001)129<0569:CAALSH>2.0.CO;2, 2001.

Chen, L., X. Zheng, J. Yang., and J. H. Yoon.: Impact of BIPV windows on building energy consumption in street canyons: Model development and validation, Energ. Buildings, 249, 11207, doi:10.1016/j.enbuild.2021.111207, 2021.

Chua, P. L. C., Takane, Y., Ng, C. F. S., Oka, K., Honda, Y., Kim, Y., and Hashizume, M.: Net impact of air conditioning on heat-related mortality in Japanese cities. Environmental International, 181, 108310. doi: 10.1016/j.envint.2023.108310, 2023.

Crawley, D. B., Lawrie, L. K., Winkelmann, F. C., Buhl, W. F., Huang, Y. J., Pedersen, C. O., Strand, R. K., Liesen, R. J., Fisher, D. E., Witte, M. J., and Clazer, J.: EnergyPlus: Creating a new-generation building energy simulation program. Energy and Buildings, 33(4), 319–331. doi: 10.1016/S0378-7788(00)00114-6, 2001.

Demuzere, M., Kittner, J., Martilli, A., Mills, G., Moede, C., Stewart, I. D., van Vliet, J., and Bechtel, B.: A global map of local climate zones to support earth system modelling and urban-scale environmental science, Earth System. Science Data, 14, 3835–3873. doi:10.5194/essd-14-3835-2022, 2022.

GDAS, N.: FNL 0.25 Degree Global Tropospheric Analyses and Forecast Grids. Research Data Archive at the National Center for Atmospheric Research; Computational and Information Systems Laboratory: Boulder, CO, USA., 2015.

Hampo, C. C., Schinasi, L. H., and Hoque, S.: Surviving indoor heat stress in United States: A comprehensive review exploring the impact of overheating on the thermal comfort, health, and social economic factors of occupants. Heliyon, 10, e25801. 10.1016/j.heliyon.2024.e25801, 2024.

Hersbach, H., and Co-authors: The ERA5 global reanalysis. Quarterly Jounal of the Royal Meteorological Society, 146 (730), 1999–20249. doi:10.1002/qj.3803, 2020.

Hirano, T., Sugawara, H., Murayama, S., and Kondo, H.: Diurnal variation of CO2 flux in an urban area of Tokyo, Scientific Online Letters On The Atmosphere, 11, 100–103, https://doi.org/10.2151/sola.2015-024, 2015.

Iacono, M. J., Delamere, J. S., Mlawer, E. J., Shephard, M. W., Clough, S. A., and Collins, W. D.: Radiative forcing by long-lived greenhouse gases: Calculations with the AER radiative transfer models. Journal of Geophysical Research – Atmosphere, 113, D13103. doi:10.1029/2008JD009944, 2008.

IEA.: The Future of Cooling. https://www.iea.org/reports/the-future-of-cooling, 2018.

IPCC: Climate Change 2023. (2023). Synthesis Report. Contribution of Working Groups I, II and III to the Sixth Assessment Report of the Intergovernmental Panel on Climate Change [Core Writing Team, H. Lee and J. Romero (eds.)]. IPCC, Geneva, Switzerland, 35-115. 10.59327/IPCC/AR6-9789291691647.

Janjic, Z. I.: The Step-Mountain Eta Coordinate Model: Further Developments of the Convection, Viscous Sublayer, and Turbulence Closure Schemes. Monthly Weather Review, 122(5), 927–945. https://doi.org/10.1175/1520-0493(1994)122<0927:TSMECM>2.0.CO;2, 1994.

https://doi.org/10.5194/egusphere-2026-1307
Preprint. Discussion started: 1 April 2026


675 Janjic, Z. I.: Nonsingular Implementation of the Mellor-Yamada Level 2 . 5 Scheme in the NCEP Meso model, National Centers for Encironmental Prediction, Office Note #437, (February), 1–61. 2001.

Khanh, D. N., Varquez, A. C. G., and Kanda, M.: Impact of urbanization on exposure to extreme warming in megacities. Heliyon, 9 (4), e15511, doi: 10.1016/j.heliyon.2023.e15511, 2023.

Kikegawa, Y., Nakajima, K., Takane, Y., Ohashi, Y., and Ihara, T., A quantification of classic but unquantified positive
680 feedback effects in the urban-building-energy-climate system. Applied Energy, 307, 118227. doi:10.1016/j.apenergy.2021.118227, 2022.

Kikegawa, Y., Genchi, Y., Yoshikado, H., and Kondo, H., Development of a numerical simulation system toward comprehensive assessments of urban warming countermeasures including their impacts upon the urban buildings' energy-demands. Applied Energy, 76(4), 449–466. doi:10.1016/S0306-2619(03)00009-6, 2003.

685 Kikegawa, Y., Tanaka, A., Ohashi, Y., Ihara, T., and Shigeta, Y.: Observed and simulated sensitivities of summertime urban surface air temperatures to anthropogenic heat in downtown areas of two Japanese Major Cities, Tokyo and Osaka. Theoretical and Applied Climatology, 117(1), 175–193. doi:10.1007/s00704-013-0996-8, 2014.

Kikegawa, Y., Nkajima, M., and Takane, Y.: Uncertainty quantification in multi-parameter and multi-physics ensemble simulations of urban climate and building energy demand using major UCM+BEMs. 12th International Conference on
690 Urban Climate, Rotterdam, The Netherlands, 7–11 Jul 2025, ICUC12-527, doi: 10.5194/icuc12-527, 2025.

Kusaka, H., and Kimura, F.: Coupling a Single-Layer Urban Canopy Model with a Simple Atmospheric Model: Impact on Urban Heat Island Simulation for an Idealized Case. Journal of the Meteorological Society of Japan, 82(1), 67–80. doi:10.2151/jmsj.82.67, 2004.

Kusaka, H., Kondo, H., Kikegawa, Y., and Kimura, F.: A Simple Single-Layer Urban Canopy Model for Atmospheric Models:
695 Comparison with Multi-Layer and Slab Models. Boundary-Layer Meteorology, 101(ii), 329–358. doi:10.1023/A:1019207923078, 2001.

Oleson, K. W., Bonan, G. B., Feddema, J., Vertenstein, M., and Grimmond, C. S. B.: An urban parameterization for a global climate model. Part I: Formulation and evaluation for two cities. Journal of Applied Meteorology and Climatology, 47(4), 1038–1060. doi:10.1175/2007JAMC1597.1, 2008.

700 Oleson, K. W., and Feddema, J.: Parameterization and surface data improvements and new capabilities for the Community Land Model Urban (CLMU). Journal of Advances in Modeling Earth Systems, 12(2), e2018MS001586. doi:10.1029/2018MS001586, 2020.

Ohashi, Y., Genchi, Y., Kondo, H., Kikegawa, Y., Yoshikado, H., and Hirano, Y.: Influence of air-conditioning waste heat on air temperature in Tokyo during summer: Numerical experiments using an urban canopy model coupled with a building
705 energy model. Journal of Applied Meteorology and Climatology, 46(1), 66–81. doi:10.1175/JAM2441.1, 2007.

Li, D., Sun, T., Yang, J., Zhang, N., Vahmani, P., and Jones A.: Structual uncertainty in the sensitivity of urban temperatures to anthropogenic heat flux. Journal of Advances in Modeling Earth Systems, 16, e2024MS004431. doi: 10.1029/2024MS004431, 2024c.

https://doi.org/10.5194/egusphere-2026-1307
Preprint. Discussion started: 1 April 2026


Li, X., Zhao, L., Qiu, Y., Oleson, K.W., and Zhou Y.: Elevated urban energy risks due to climate-driven biophysical feedbacks. Nature Climate Change, 14, 1056–1063. doi:10.1038/s41558-024-02108-w, 2024a.

Li, X., Zhao, L., Oleson, K.W., Zhou Y., Qin, Y., Zharg, K. and Fang, B.: Enhancing urban climate-energy modeling in the Community Earth System Model (CESM) through explicit representation of urban air-conditioning adoption. Journal of Advances in Modeling Earth Systems, 16, e2023MS004107. doi:10.1029/2023MS004107 , 2024b.

Lipson, M., Grimmond, C. S. B., Best, M., Abramowitz, G., Coutts, A., Tapper, N., Baik, J.-J., Beyers, M,. Blunn, L., Boussetta, S., Bou-Zeid, E., De Kauwe, M. G., de Munck, C., Demuzere, M., Fatichi, S., Fortuniak, K., Han, B.-S., Hendry, M., Kikegawa, Y., Kondo, H., Lee, D.-Il, Lee, S.-H., Lemonsu, A., Machado, T., Manoli, G., Martilli, A., Masson, V., McNorton, J., Meili, N., Meyer, D., Nice, K. A., Oleson, K. W., Park, S.-B., Roth, M., Schoetter, R., Simón-Moral, A., Steeneveld, G.-J., Sun, T. Takane, Y., Thatcher, M., Tsiringakis, A., Varentsov, M., Wang, C., Wang, Z.-H., and Pitman, A.: Evaluation of 30 urban land surface models in the Urban-PLUMBER project: Phase 1 results. Quarterly Journal of the Royal Meteorological Society, 150, 126–169. doi:10.1002/qj.4589, 2023.

Loridan, T., Lindberg, F., Jorba, O., Kotthaus, S., Grossman-Clarke, S., and Grimmond, C. S. B.: High resolution simulation of the variability of surface energy balance fluxes across centoral London with urban zones for energy partitioning. Boundary–Layer Meteorology, 147, 493–523. doi:10.1007/s10546-013-9797-y, 2013.

Meili, N., Manoli, G., Burlando, P., Bou-Zeid, E., Chow, W. T., Coutts, A. M., Daly, E., Nice, K. A., Roth, M., Tapper, N. J., Velasco, E., Vivoni, E. R., and Fatichi S.: An urban ecohydrological model to quantify the effect of vegetation on urban climate and hydrology (UT&C v1.0), Geoscientific Model Development, 13, 335–362. doi: 10.5194/gmd-13-335-2020, 2020.

Meili, N., Zheng, X., Takane, Y., Nakajima, K., Yamaguchi, K., Chi, D., Zhu, Y., Wang, J., Qiu, Y., Paschalis, A., Manoli, G., Burlando, P., Puay Yok, T., and Fatichi, S.: Modeling the effect of trees on energy demand for indoor cooling and dehumidification across cities and climates. Journal of Advances in Modeling Earth Systems, 17, e2024MS004590. doi: 10.1029/2024MS004590, 2025.

Mellor, G. L., and Yamada, T., Development of a Turbulence Closure Model for Geophysical Fluis Problems. Reviews of Geophysics and Space Physics, 20(4), 851–875. doi:10.1029/RG020i004p00851, 1982.

Morrison, H., Thompson, G., and Tatarskii, V.: Impact of cloud microphysics on the development of trailing stratiform precipitation in a simulated squall line: Comparison of one- and two-moment schemes. Monthly Weather Review, 137(3), 991–1077. doi:10.1175/2008MWR2556.1, 2009.

Nakajima, K., Takane, Y., Fukuba, S., Yamaguchi, K., and Kikegawa, Y.: Urban electricity–temperature relationships in the Tokyo Metropolitan Area. Energy and Buildings, 256, 111729. doi:10.1016/j.enbuild.2021.111729, 2022.

Nakajima, K., Takane, Y., Kikegawa, Y., Furuta, Y., and Takamatsu, H.: Human behaviour change and its impact on urban climate: Restrictions with the G20 Osaka Summit and COVID-19 outbreak. Urban Climate, 35, 100728. doi:10.1016/j.uclim.2020.100728, 2021.

https://doi.org/10.5194/egusphere-2026-1307
Preprint. Discussion started: 1 April 2026


Nakajima, K., Takane, Y., Kikegawa, Y. and Yamaguchi, K.: Improvement of WRF–CM–BEM and its application to high-resolution hindcasting of summertime urban electricity consumption. Energy and Buildings, 296, 113336. doi:10.1016/j.enbuild.2023.113336, 2023.

Niu, G ., Yang, Z.–L., Mitchell, K. E., Chen, F., Ek, M. B., Barlage, M., Kumar, A., Manning, K., Niyogi, D., Rosero, E., Tewari, M., and Xia, Y.: The community Noah land surface model with multiparameterization options (Noah–MP): 1. Model description and evaluation with local–scale measurements. J. Geophys. Res. Atmos., 116,D12109, doi:10.1029/2010JD015139, 2011.

Robine, J. M., Cheung, S. L., Le Roy, S., Van Oyen, H., Griffiths, C., Michel, J. P., and Herrmann, F. R. : Death toll exceeded 70,000 in Europe during the summer of 2003. Comptes rendus biologies, 331, 171–178. doi:10.1016/j.crvi.2007.12.001, 2008.

Salamanca, F., Georgescu, M., Mahalov, A., Moustaoui, M., and Wang, M.: Anthropogenic heating of the urban environment due to air conditioning. Journal of Geophysical Research: Atmospheres, 119(10), 5949–5965. doi:10.1002/2013JD021225, 2014.

Salamanca, F., Krpo, A., Martilli, A., and Clappier, A.: A new building energy model coupled with an urban canopy parameterization for urban climate simulations—part I. formulation, verification, and sensitivity analysis of the model. Theoretical and Applied Climatology, 99(3–4), 331–344. doi:10.1007/s00704-009-0142-9, 2010.

Skamarock, W. C., Klemp, J. B., Dudhia, J., Gill, D. O., Liu, Z., Berner, J., … Huang, X. -yu.: A Description of the Advanced Research WRF Model Version 4.3 (No. NCAR/TN-556+STR). doi:10.5065/1dfh-6p97, 2021.

Sugawara, H., Ishidoya, S., Terao, Y., Takane, T., Kikegawa, Y., and Nakajima, K.: Anthropogenic $CO_2$ emissions changes in an urban area of Tokyo, Japan due to the COVID-19 pandemic: A case study during the state of emergency in April–May 2020, Geophys. Res. Lett., 48, e2021GL092600, https://doi.org/10.1029/2021GL092600, 2021.

Sun, M., Pan, J., Zhao, Q., and Bardhan, R.: Heat stress dichotomy: long-term adaptation and acute shock in London domestic environments. Phil. Trans. R. Soc. A, 383(2308), 20240567. doi:10.1098/rsta.2024.0567, 2025.

Sun, Y., Takane, Y., Yamaguchi, K., and Ihara, T.: The photovoltaic heat island effect in Tokyo: Morphological dependence and spatiotemporal dynamics of PV-induced urban warming. Building and Environment, 288, 113941. doi: 10.1016/j.buildenv.2025.113941, 2026.

Takane, Y., and Kikegawa, Y.: WRF–SLUCM+BEM (v2.0) source code for GMD submission. Zendo [code]. doi: 10.5281/zenodo.18918749, 2026.

Takane, Y., Kikegawa, Y., Nakajima, K., and Kusaka, H.: SLUCM+BEM (v1.0): a simple parameterisation for dynamic anthropogenic heat and electricity consumption in WRF-Urban (v4.3.2). Geoscientific Model Development, 17, 8639-8664. doi: 10.5194/gmd-17-8639-2024, 2024a.

Takane, Y., Kikegawa, Y., Nakajima, K., and Kusaka, H.: WRF–SLUCM+BEM: Input data for the evaluation at Tokyo Metropolitan Area. Zendo [data set]. doi:10.5281/zenodo.10685693, 2024b

https://doi.org/10.5194/egusphere-2026-1307
Preprint. Discussion started: 1 April 2026


Takane, Y., Kikegawa, Y., and Kusaka, H.: WRF–SLUCM+BEM source code for GMD submission. Zendo [code]. doi: 10.5281/zenodo.10686465, 2024c.

Takane, Y., Kikegawa, Y., Hara, M., Ihara, T., Ohashi, Y., Adachi, S. A., et al.: A climatological validation of urban air temperature and electricity demand simulated by a regional climate model coupled with an urban canopy model and a building energy model in an Asian megacity. International Journal of Climatology, 37(1), 1035–1052. doi:10.1002/joc.5056, 2017.

Takane, Y., Kikegawa, Y., Hara, M., and Grimmond, C. S. B.: Urban warming and future air-conditioning use in an Asian megacity : importance of positive feedback. NPJ Climate and Atmospheric Science, 2, 39. doi:10.1038/s41612-019-0096-2, 2019.

Takane, Y., Nakajima, K., Yamaguchi, K., and Kikegawa, Y.: Decarbonisation technologies can halve the nonlinear increase in electricity demand in densely populated areas due to climate change. Sustainable Cities and Society, 99, 104966. doi:10.1016/j.scs.2023.104966, 2023a.

Takane, Y., Nakajima, K., and Kikegawa, Y.: Urban climate changes during the COVID-19 pandemic: integration of urban-building-energy model with social big data. NPJ Climate and Atmospheric Science, 5, 44. doi:10.1038/s41612-022-00268-0, 2022.

Takane, Y., Ohashi, Y., Grimmond, C. S. B., Hara, M., and Kikegawa, Y.: Asian megacity heat stress under future climate scenarios: impact of air-conditioning feedback. Environmental Research Communications, 2, 015004. doi:10.1088/2515-7620/ab6933, 2020.

Takane, Y., Nakajima, K., Kikegawa, Y., and Yamaguchi, K.: Enhancing urban canopy building energy models through the integration of social big data: Improvement and application, International Association for Urban Climate (IAUC) Urban Climate News, 89, 17–21, 2023b.

Tsiringakis, A., Holtslag, A. A. M., Grimmond, C. S. B., and Steeneveld, G. J.: Surface and atmospheric driven variability of the Single-Layer Urban Canopy Model under clear-sky conditions over London. Journal of Geophygical Research Atmosphere, 125, e2019JD032167. doi: 10.1029/2019JD032167, 2020.

Tsiringakis, A., Steeneveld, G.-J., Holtslag, A. A. M., Kotthaus, S., and Grimmond, C. S. B.: On- and off-line evaluation of the single-layer urban canopy model in London summertime conditions. Quarterly Journal of the Royal Meteorological Society, 145, 1474–1489. doi: 10.1002/qj.3505, 2019.

Varquez, A.C.G., Kiyomoto, S., Khanh, D.N., and Kanda, M.: Global 1-km present and future hourly anthropogenic heat flux. Sci Data 8, 64, doi: 10.1038/s41597-021-00850-w, 2021.

Yamasaki, L., Kamada, T., Ng, C. F. S., Takane, T., Nakajima, K., Yamaguchi, K., Oka, K., Kim, Y., and Hashizume, M.,: Heat-related mortality and ambulance transport after a power outage in the Tokyo metropolitan area. Environmental Epidemiology, 8, e292. doi: 10.1097/EE9.0000000000000292, 2024.

https://doi.org/10.5194/egusphere-2026-1307
Preprint. Discussion started: 1 April 2026


Yang, J., Wang Z.-H. , Chen F. , Miao S. , Tewari M. , Voogt J. , and Myint S.,: Enhancing hydrologic modelling in the coupled Weather Research and Forecasting–urban modelling system. Bound.-Layer Meteor., 155, 87–109, doi:10.1007/s10546-014-9991-6. 2015.

Yang, J., Wang, Z.-H., Georgescu, M., Chen, F., and Tewari, M: Assessing the impact of enhanced hydrological processes on urban hydrometeorology with application to two cities in contrasting climates. Journal of Hydrometeorology, 17, 1031–1047. doi:10.1175/JHM-D-15-0112.1, 2016.

Zonato, A., Martilli, A., Gutierrez, E., Chen, F., He, C., Barlage, M., Zardi, D., and Giovannini, L: Exploring the effects of rooftop mitigation strategies on urban temperatures and energy consumption. J. Geophys. Res. Atmos., 126 (21), e2021JD035002, doi:10.1029/2021JD035002, 2021.

Zhao, L., Lee, X., Smith, R. B, and Oleson, K,: Strong contributions of local background climate to urban heat islands. Nature, 511, 216–219. doi:10.1038/nature13462, 2014.

Zhao, Q., Hu, C., Ou, Y., Livingston, M., Wang, M., Hamada, R., and Eccles, P.: Sensor-enhanced housing survey data for urban heat investigation in Southwark, London [Data set]. Zenodo. https://doi.org/10.5281/zenodo.14444475, 2023.